

**SPECTRAL CHARACTERISTICS OF SOME PRACTICAL
VARIATIONS IN THE HALF-SINE AND SAWTOOTH PULSES**

EDWARD H. SCHELL

613024

FOREWORD

This report was prepared in the Environmental Control Branch of the Vehicle Equipment Division, Air Force Flight Dynamics Laboratory, under Project No. 1309, "Environmental Interactions," Task No. 130904, "Induced Environmental Interactions."

The report covers work conducted from 1 February to 1 August 1964.

The author wishes to acknowledge the very significant contributions of Ernst Tolle, Joseph Marous, John Sansom, and Dave La Jeunesse.

This technical report has been reviewed and is approved.



T. J. BAKER

Asst. for Research and Technology
Vehicle Equipment Division

ABSTRACT

This report deals with shock analysis and design as they affect equipment. Considered in the analysis is a two part function composed of a ramp tangent to a half-sine pulse in which the rise times and decay times can be controlled independently of each other. Such a pulse is more representative of the physical condition present in a partially plastic, partially elastic shock machine such as the lead pellet types. The pulse is changed by increments from an ideal terminal peak sawtooth to an ideal half-sine.

Positive and negative response spectra with a range of damping from zero to critical are presented. Fourier spectra are also presented.

Insofar as is known, this is the first time these test pulses have been studied in such detail. The data presented should prove quite useful for designers using several response spectrum or Fourier spectrum techniques for design problems resulting from sawtooth or half-sine shock tests. The report shows an important type of modal interaction failure which cannot be adequately excited with a symmetrical waveform even if testing is accomplished in both directions.

TABLE OF CONTENTS

SECTION	PAGE
INTRODUCTION	1
SELECTION OF THE ANALYTICAL FUNCTION	2
SHOCK RESPONSE SPECTRA	5
FOURIER SPECTRA	7
CRITERION FOR PROXIMITY FAILURES	9
SAWTOOTH VERSUS HALF-SINE	11
CONCLUSIONS	12
REFERENCES	13
APPENDIX: FORMULAS AND TABLES	15
Point of Tangency of the Ramp-Sine Function	15
Determination of Area of Ramp-Sine Function	15
Alternate Excitations and Responses	16

ILLUSTRATIONS

FIGURE	PAGE
1. Ideal Sawtooth Spectra (After Morrow, Reference 4)	19
2. (a) Triangular Function Used in Previous Studies	20
(b) Ramp-Sine Function Studied in This Report	20
3. Test Setup and Schematic Representation	21
4. Comparison of a Record of an Actual Test Pulse With an Ideal Terminal Peak Sawtooth Pulse	22
5. Ramp-Sine Pulses	23
6. Half-Sine Response Spectra for $T_R/T = .5$	24
7. Ramp-Sine Response Spectra $T_R/T = .556$	25
8. Ramp-Sine Response Spectra for $T_R/T = .625$	26
9. Ramp-Sine Response Spectra for $T_R/T = .758$	27
10. Ramp-Sine Response Spectra for $T_R/T = .870$	28
11. Ramp-Sine Response Spectra for $T_R/T = .909$	29
12. Ramp-Sine Response Spectra for $T_R/T = 1.000$	30
13. Variations in Response Spectra for $\zeta = 0$	31
14. Variations in Response Spectra for $\zeta = 0.1$	32
15. Variations in Response Spectra for $\zeta = 0.5$	33
16. Variations in Response Spectra for $\zeta = 1.0$	34
17. Fourier Amplitude and Phase Spectra for $T_R/T = .500$	35
18. Fourier Amplitude and Phase Spectra for $T_R/T = .556$	36
19. Fourier Amplitude and Phase Spectra for $T_R/T = .625$	37
20. Fourier Amplitude and Phase Spectra for $T_R/T = .758$	38
21. Fourier Amplitude and Phase Spectra for $T_R/T = .870$	39
22. Fourier Amplitude and Phase Spectra for $T_R/T = .909$	40
23. Fourier Amplitude and Phase Spectra for $T_R/T = 1.000$	41

ILLUSTRATIONS (Continued)

FIGURE	PAGE
24. Variations in Fourier Amplitude and Phase Spectra	42
25. Fourier Real and Imaginary Spectra for $T_R/T = .500$	43
26. Fourier Real and Imaginary Spectra for $T_R/T = .556$	44
27. Fourier Real and Imaginary Spectra for $T_R/T = .625$	45
28. Fourier Real and Imaginary Spectra for $T_R/T = .758$	46
29. Fourier Real and Imaginary Spectra for $T_R/T = .870$	47
30. Fourier Real and Imaginary Spectra for $T_R/T = .909$	48
31. Fourier Real and Imaginary Spectra for $T_R/T = 1.000$	49
32. Variations of the Fourier Real and Imaginary Spectra	50
33. Model Equipment for Determining Proximity Failure Criteria for a Given Excitation	51
34. Proximity Criteria for Half-Sine and Sawtooth Pulses When the Half- Sine Criterion is Near Zero	52
35. Proximity Criteria for Half-Sine and Sawtooth Pulses When the Half- Sine Criterion is Near Maximum	53

SYMBOLS

A	peak value of an excitation
B	ordinate of the point of tangency of the ramp-sine function as shown in Figure 2b
c	viscous damping coefficient
D	proximity, (derivation in text)
D_{st}	static value of D, (see text)
e	base of Napierian logarithms (2.7183)
E	generalized excitation
f	general function of a specific variable
f	cyclic frequency
F	complex Fourier spectrum
I	the imaginary part or component (b) of the complex number $a + jb$
j	$\sqrt{-1}$
K	stiffness
M	mass
m	subscript meaning "the maximum value of"
n	0, 1, 2, 3 ---etc.
p	subscript meaning "the peak value of"
R	generalized response of a linear single-degree-of-freedom system
R	the real part or component (a) of the complex number $a + jb$
t	instantaneous time
t_d	duration of an excitation time function
T	duration of an excitation time function
T_R	time of rise to the peak value of an excitation
T_1	abscissa of the point of tangency of the ramp-sine function as shown in Figure 2b

SYMBOLS (Continued)

u	absolute displacement excitation
x	absolute displacement response
δ	relative displacement response
Δ	proximity criterion (derivation in text)
ζ	fraction of critical damping
ϕ	phase difference of Fourier amplitude components
ω	angular frequency
ω_n	angular natural frequency

INTRODUCTION

Much has been written concerning the advantages of a terminal peak sawtooth wave for shock testing and design purposes (References 1-4). The superiority of the waveform is demonstrated by showing the undamped positive and negative acceleration shock spectra. These spectra tend to be nearly constant above some selectable frequency as shown in Figure 1, and the negative values are equal to the positive values. The latter feature has been used to justify testing in only one direction along each of the three principal axes of the equipment.

An important point was demonstrated by Lowe and Cavanaugh (Reference 2) when they studied an actual test pulse and were able to show that practical shock machine pulses are not quite as superior as would be indicated by the spectrum of the theoretically perfect sawtooth. They used the work of Jacobsen and Ayre (References 5, and 6) to explain their results on a theoretical basis. This work shows that a finite drop-off time (rather than zero drop-off time as in the theoretically perfect pulse) results in a reduction of the magnitudes of the residual (and hence the negative) undamped spectrum particularly at higher frequencies. The pulse studied by Jacobsen and Ayre was a triangular pulse with a rise time independent of the drop-off time. This pulse, shown in Figure 2a is useful in studying the responses of equipments to a sawtooth test because it retains most of the essential features of the shock. None of the previous references, however, have considered the effects of damping, which are always present in a realistic system. A report by Luke (Reference 7) of the University of Texas considers the effect of damping on the positive response spectrum of the theoretically perfect sawtooth. The negative response spectrum, and practical deviations from the theoretically perfect waveform, however, were not studied. Since both damping and drop-off time exert a different (and much larger) influence on the negative response spectrum, a gap in our knowledge exists in this area.

All of the previous studies used analytical functions which are only partially justifiable on the basis of physical reality, that is, the analytical pulse does not look like the oscillogram of an actual test pulse nor can it be fully justified by reasoning from the physical phenomena present during the actual test.

In the past few years several publications (References 6, 8, and 9) have dealt with the application of the Fourier transform to shock analysis and design problems. Painter and Parry (Reference 10) have applied Fourier spectrum techniques to the problem of laboratory simulation of the shock environment. It has also been suggested that the Fourier spectrum be used as a means of specifying shock test conditions (Reference 11). Morrow (Reference 12) regards the Fourier spectrum as a more fundamental analytical tool and suggests that it may eventually supersede the shock spectrum for purposes of data reduction.

In view of the foregoing discussion, it was decided to undertake an effort designed to bring increased agreement between theoretical and practical results and to provide design information to be used in several different design methods. This was to be accomplished by selection of an analytical function with variable characteristics and reduction of the pulse to damped and undamped positive and negative shock spectra and to complex Fourier spectra for variations of the function over a given range of values of the ratio of the rise time to the drop-off time.

After the function was selected, it became apparent that the function could also be used to study the effects of distortion on the half-sine pulse and to study the effects of symmetry and asymmetry as represented by the half-sine and terminal peak sawtooth waveforms. These studies were also included.

Finally, the work was expanded to include demonstration of the superiority of the terminal peak sawtooth waveform for testing purposes when the failure criterion is the proximity or collision of two uncoupled simple systems.

Designers can make direct use of the pulse in the solution of preliminary design problems when the differential equations of motion of the system can be written, or with the convolution (Du Hamel's) integral for simple linear systems. These design methods are covered by most of the standard shock and vibration texts (References 4-6, and 13-16) and engineering mathematics (References 17 and 18) texts. The pulse may also be used with phase-plane graphical techniques for the solution of a wide variety of linear and non-linear, single and multi-degree-of-freedom problems including various types of damping (References 5, 6, and 19). The shock spectra may be used directly if the system can be considered to behave as a linear single-degree-of-freedom system or they may be used with normal mode theory (References 20-23) for more complex systems. The Fourier spectra may be used with a hypothetical transfer function in the preliminary design of linear systems. When the design reaches the hardware stage, the actual transfer function can be measured for use with the spectra. A recent paper by Mains (Reference 9) thoroughly explores Fourier design techniques. Several other publications (References 6, 8, and 15) also treat the subject.

SELECTION OF THE ANALYTICAL FUNCTION

Theoretically, it is possible to produce shaped pulses which decay from a peak value to one g in zero time on a free-fall shock machine. This is done by dropping a perfectly rigid table onto a shaped plastic pellet resting on an infinitely massive perfectly rigid anvil. All of the kinetic energy of the table is absorbed by plastic deformation of the pellet. At the instant when all of the kinetic energy has been dissipated in doing work to deform the pellet, the acceleration will drop instantaneously to one g .

In a practical machine using a lead pellet as the plastic element, the ideal pulse is unobtainable due to elasticity in the pellet and elements of the machine. This is illustrated graphically in Figure 3. The figure represents the major elements of the shock machine and the pellet after the shock is over and the elements shown are at rest. The test setup is shown schematically as a lumped parameter system consisting of masses and linear elastic elements. This is because the table and anvil are not perfectly rigid, that is, K_2^* and K_4 are not infinite, and the lead pellet is not perfectly plastic but also exhibits elasticity K_3 . Thus the pulse generation system is partially plastic and partially elastic.

The waveform for a perfectly elastic linear system has been shown many times to be a perfect half-sine. During this pulse the free-fall velocity is reduced to zero at the peak of the pulse and then increased to the initial value in the opposite direction at the end of the pulse causing a rebound to the original drop height because elastic systems do not

*See list of symbols

dissipate energy. During the rising portion of the pulse, the elastic element completely converts the kinetic energy of the free-falling table and test item into potential energy stored in the spring at the peak acceleration. During the unloading portion of the pulse, the stored energy is returned to the table and test item increasing their kinetic energy to the original value. The timing of events during the pulse is a function of the falling mass and the spring rate.

Figure 4 shows the results of this partially elastic pulse generation mechanism in a photograph of an actual machine generated terminal peak sawtooth pulse. A superposed ideal sawtooth pulse is included for comparison. This pulse was generated with a lead pellet on a standard, commercially available, gravity-powered impact machine.

The actual terminal peak sawtooth test pulse differs from the theoretical pulse in the following ways:

- (a) The rising portion is not quite linear, although this pulse is exceptionally good in this respect. (Pulses, normally, are more nonlinear).
- (b) There are no discontinuities in the pulse, especially at the peak which rounds smoothly into the decaying portion of the curve.
- (c) A finite drop-off time is exhibited in the unloading portion of the pulse after the peak is reached.
- (d) A high frequency low amplitude oscillation appears at the end of the pulse. The frequency is approximately 1750 cps.

These observable differences are explained as follows:

(a) The linearity of the rising portion of the pulse is a function of the pellet shape. With some effort, the rising portion can be made more linear by redesign of the pellet. The results, however, may not be worth the effort.

(b) Physically generated pulses never exhibit discontinuities. The rounding at the peak is attributed to the partial elasticity of the generation system.

(c) Any system with elasticity requires time to unload. During the drop-off era, the table and test item are being accelerated in a vertically upward direction due to the release of the energy stored in the elastic elements. The table then rebounds as a result of the upward acceleration. This is the same physical condition present in the generation of a half-sine shock pulse with a linear spring and the unloading portion of the pulse appears to be nearly a quarter-sine as it is with the half-sine pulse.

(d) The structural ringing at the end of the pulse is associated with the predominant natural mode of the test machine. This structural response is excited by the high rate-of-change of the acceleration (jerk) in the drop-off. This may or may not have important consequences depending on the frequencies and amplitudes involved and also the test item. Since this problem is a very specific problem, it cannot be treated as part of a generalized analytic function without vastly multiplying the complexity of the study. In future work, it is believed that the "tail-wagging" on the pulse can be handled as a separate damped sinusoid using super-position methods. This aspect will not be treated in this paper.

Although the previous discussion refers to the lead-pellet terminal peak sawtooth pulse, some elasticity is a characteristic of all methods of pulse generation. As a result, all practical sawtooth pulses have a rounded peak and require a finite drop-off time. An analytical function based on the previous development will, therefore, have general applicability.

The selected pulse is shown in Figure 2b. It has all the essential features of the actual test pulse except the structural ringing at the end. It is composed of a ramp tangent to a half-sine. The analytical statement of the function is as follows:

$$\begin{aligned}
 f(t) &= f_1(t) + f_2(t) \\
 f_1(t) &= Bt/T_1 && 0 \leq t \leq T_1 \\
 f_1(t) &= 0, && t \leq 0, T_1 < t \\
 f_2(t) &= A \sin \frac{\pi(t - 2T_R + T)}{2(T - T_R)}, && T_1 \leq t \leq T, T_R \neq T \\
 f_2(t) &= 0, && t < T_1, T \leq t
 \end{aligned}$$

In addition to the physical significance, the ramp-sine function has several other niceties which make it useful for a variety of present and future studies:

(a) When T_R and T are equal, the function is a theoretically perfect terminal peak sawtooth.

(b) When T_R equals half of T , the function is a theoretically perfect half-sine.

(c) If the function is defined for negative values of time, when T_R is equal to T , the function is a theoretically perfect initial peak sawtooth.

(d) When the function is defined for negative values of T , it is the mirror image of the function defined for positive values of T .

These features make it possible to vary the function incrementally from an initial peak sawtooth through a half-sine to a terminal peak sawtooth by varying the ratio of T_R to T .

The present paper considers only positive values of time. Some of the pulses studied are shown in Figure 5. In addition to these, spectra of one other pulse are presented in this paper. It has a T_R to T ratio of .909 and represents the condition of maximum decay for the nominal 10 millisecond shocks of MIL-STD-810A. The nominal 6 millisecond shock of MIL-STD-810A is covered by the pulse with a T_R to T ratio of .870. Minimum duration times for these tests are given by the ideal case where the T_R to T ratio is 1.0.

SHOCK RESPONSE SPECTRA

The response spectra were computed on a digital computer by determining the generalized response R from the generalized second order linear differential equation of a single-degree-of-freedom system. This equation was developed by Professor Ayre (Reference 6) and is quite useful.

$$\frac{\ddot{R}}{\omega_n^2} + \frac{2\zeta \dot{R}}{\omega_n} + R = E$$

The advantages of this generalized form are discussed in a previous paper (Reference 24). A table of specific excitations and responses is included in the appendix of this paper for those who are interested in the responses of systems to a pulse of this shape for other motional parameters as well as acceleration. The specific excitation used for this problem is the acceleration time function \ddot{u} . The specific differential equation then becomes:

$$-\ddot{\delta} - 2\zeta \omega_n \dot{\delta} - \omega_n^2 \delta = \ddot{u}$$

where δ is the relative displacement. Conversion of the generalized response to the specific response is as follows: $R = -\omega_n^2 \delta$. The response spectra are shown in Figures 6 through 12. The ordinates are in the normalized general form:

$$\frac{R_m}{E_p} = \frac{-\omega_n^2 \delta_m}{\ddot{u}_p}$$

where the subscripts m and p refer to the maximum and peak values. The abscissa is the normalized product fT where f is the natural frequency of the responding system and T is the time length of the excitation function. Each curve represents a different damping ratio ζ .

The maximum relative displacement response is obtained from the previous relationship:

$$\delta_m = \frac{-\ddot{u}_p}{\omega_n^2} \left(\frac{R_m}{E_p} \right)$$

These spectra were computed for comparison on the basis of equal amplitudes and equal durations based on the assumption that it is much easier for a test engineer to control the peak value and duration of a specified shock motion than it is to match the specified shape. The study, therefore, was aimed primarily at showing the effects of deviation from specified shapes.

Examination of the ideal sawtooth spectra of Figure 12 indicates that the addition of damping smoothes out the ripples in the spectrum. It is also seen that damping has a greater effect in reducing negative responses than it does in reducing positive responses.

Finally, the figure shows that the undamped negative responses are between 31 percent and 54 percent larger than the damped negative responses for $\zeta = 0.1$. This amount of damping is rather common for equipment on isolators or for equipment with damping intentionally built into it to control vibration responses. Such an amount of damping may also be unintentionally present due to the use of plastic and elastomeric insulation or other materials as well as coulomb damping between parts.

Figure 10 shows the spectra of a pulse which meets the requirements for the nominal 6 millisecond pulse of MIL-STD-810. It is seen that the undamped negative response at $fT = 4.0$ is somewhat less than that shown in the ideal case. The undamped negative response in the ideal case is 23 percent greater. The ideal case is 82 percent greater than the response for $\zeta = 0.1$. This frequency is 581 cps. If we extrapolate to 1000 cps, the undamped negative spectrum for the ideal case is approximately 100 percent greater than the undamped negative spectrum of the assumed test pulse. At 1000 cps the undamped negative response for the ideal pulse is approximately 300 percent greater than the damped negative response for the condition $\zeta = 0.1$ for the assumed test pulse.

The point of these comparisons of assumed test spectra with the undamped negative spectra of the ideal terminal peak sawtooth is to emphasize the fallacy of testing in only one direction along each of the 3 principal axes of the equipment. In other words, the assumption that positive and negative responses for a terminal peak sawtooth test are equal is justifiable only under certain highly restricted circumstances.

Response spectra for the ideal half-sine case are shown in Figure 6. Damped positive and negative half-sine spectra were previously presented by Shapiro and Hudson (Reference 25) and Rubin (Reference 6). They were recomputed for comparison purposes for this study. The most important feature of these spectra are the low values in the negative spectra and the nulls or tendencies to nulls in the negative spectra at fT values of $1.5 + n$. Jacobsen and Ayre (Reference 5) have shown these nulls to be a characteristic of symmetrical pulses. It is also interesting to note that the addition of damping up to some maximum value increases the negative responses at these nulls. Increasing damping beyond this value causes a decrease in the negative responses until they become zero for critical damping. Examination of the positive spectra of Figures 7 through 12 indicates that an analogous condition is also present in the positive spectra.

Summary plots for each of the four values of damping are presented in Figures 13 through 16. These graphs can be used for interpolation and extrapolation of the responses to a ramp-sine function of any T_R/T ratio. The first of these figures shows the undamped case. The following points can be deduced from the figure:

(a) In the impulsive behavior region where fT is less than .25, the responses in both the positive and negative spectra are equal, except for sign, and the differences due to a change of T_R/T are at a minimum. The actual differences are proportional to the differences in the areas of the excitation functions.

(b) The positive spectrum between $fT = .25$ and 2.0 is sensitive to changes of T_R/T . This is due to the combined effects of changes in shape and area of the excitation function.

(c) The region above $fT = 2$ is approximately unity in the positive spectrum which indicates that this area is relatively insensitive to the ratio of T_R/T .

(d) The negative spectrum is quite sensitive to changes in T_R/T for values greater than $fT = .25$ with the single exception of values of fT near 1.2 where the values tend to be nearly equal and nearly unity for all exciting functions. Since T_R/T is a measure of the degree of symmetry present in the excitation function, it is evident that the effects of the degree of symmetry are more pronounced in the negative spectrum.

The same general statements apply to the case for a damping ratio of .1 shown in Figure 14 except that sensitivities to differences of T_R/T have been somewhat deemphasized by the addition of damping.

When the damping ratio is .5, as shown in Figure 15, the negative portion of the spectrum tends to become insignificant while the positive portion tends to be relatively insensitive to changes of T_R/T throughout the spectrum.

The final case considered is for critical damping. This case is shown in Figure 16. Since the definition of critical damping implies a minimum response of zero, there is no negative spectrum. The positive portion of the spectrum is even more insensitive than the previous case.

FOURIER SPECTRA

The Fourier spectra were computed from the Fourier integral as follows:

$$F(\omega) = \int_0^T f(t) e^{-j\omega t} dt$$

$$F(\omega) = \int_0^T f(t) \cos \omega t dt - j \int_0^T f(t) \sin \omega t dt$$

$$F(\omega) = R[F(\omega)] + j I[F(\omega)]$$

This equation provides data for the Fourier real and imaginary spectra. They are sometimes referred to as the cosine and sine spectra respectively.

An alternative form of the Fourier spectrum which is preferred by some engineers is:

$$F(\omega) = |F(\omega)| e^{j\phi(\omega)}$$

$$|F(\omega)| = \{ R^2 [F(\omega)] + I^2 [F(\omega)] \}^{1/2}$$

$$\phi(\omega) = \tan^{-1} \frac{I[F(\omega)]}{R[F(\omega)]}$$

The latter two equations provide data for the Fourier amplitude and phase spectra. Since both methods of presenting the spectra are useful, the small effort required to present them in both ways was considered worthwhile.

The Fourier amplitude and phase spectra are shown in Figures 17 through 23. The abscissa is normalized for general applicability by multiplying the frequency of the Fourier component by the pulse duration. The ordinate values are normalized by dividing by the value of $F(\omega)$ at $\omega = 0$. This is merely the area of the forcing function. The

values of $|F(\omega)|$ for any ramp-sine function can be interpolated by knowing the peak value of the function A , the duration T , and the rise time T_R . Values of $F(0)/AT$ can be interpolated from Table 1 of the Appendix. From these, $|F(\omega)|$ is obtained by multiplying the ordinate by $F(0)/AT$ from the table and the known amplitude and duration AT . The frequency f is obtained by dividing the abscissa by T . Phase angles $\phi(\omega)$ are determined directly from the curves. Examination of the half-sine spectra of Figure 17 indicates that zeros of the absolute value occur at $1.5 + n$. This is to be expected since the undamped residual shock spectrum is related to the Fourier spectrum by the constant frequency factor ω_n and these zeros were observed in the undamped shock spectrum. It is also seen that phase discontinuities exist wherever these zeros exist. These can be shown to be true discontinuities since the sine of the angle is discontinuous at the same point.

In the other phase spectra, apparent discontinuities are seen. These, however, are not true discontinuities. They are merely the result of plotting the phase as an angle between 0 and 2π radians. It can be shown that the tangent of the phase angle at an apparent discontinuity is continuous. Therefore, the phase angles must also be continuous at the apparent discontinuity. Because the Fourier components exist forever, it can be shown that the phases of the components can be described by any angle which is different from $\phi(\omega)$ by the angle $\pm 2n\pi$.

A close study of the results obtained in the spectra of Figures 17 through 23 has not been attempted. However, it is obvious that major characteristics of the phase spectrum can be correlated with major characteristics of the amplitude spectrum. For example, the half-sine pulse shows discontinuities in the phase spectrum at the same frequencies that zeros occur in the amplitude spectrum. In Figure 18, the points of maximum curvature and points of inflection of the phase spectrum occur at odd and even multiples of $\pi/2$ respectively and seem to be related to some corresponding point (as of now undetermined) in the amplitude spectrum. This suggests the possibility that the phase spectrum may be determined from the amplitude spectrum. Since the Fourier integral can be inverted to obtain the time history, this in turn implies the possibility of inversion of the undamped residual shock spectrum since it fully determines the Fourier amplitude spectrum. No conclusions will be made on this subject and it is reserved for future study.

A summary plot of the amplitude and phase spectra is shown in Figure 24. Examination of the amplitude spectrum shows the low frequency values to be close together below $fT = 1.0$. At $fT = 0$, all values converge to unity. This could have been predicted from the shock spectra.

The extreme effect of asymmetry, as represented by the sawtooth case $T_R/T = 1.0$, is to smooth out the spectra, both amplitude and phase. The extreme effect of symmetry, as represented by the half-sine case $T_R/T = .5$, is the introduction of discontinuities in both the amplitude and phase spectra. Intermediate cases provide a smooth transition from one extreme to the other. The case $T_R/T = .556$ is particularly interesting since it shows a rather large variation in the phase spectrum as it approaches the discontinuous spectrum of the symmetrical function $T_R/T = .5$.

The normalized real and imaginary spectra are plotted in Figures 25 through 31. The values of the real and imaginary parts can be determined by multiplying the ordinate by the value of $F(0)/AT$ from Table 1 of the appendix and the known value of A and T . The frequency is determined by dividing fT by T as before.

In general, the greater the symmetry, the smoother the spectra, both real and imaginary. This is most evident at the higher frequencies.

It is interesting to note that the real part of the half-sine case $T_R/T = .5$ is negative for all values of fT greater than .5.

A summary plot of real and imaginary spectra is shown in Figure 32. At the lower frequencies the curves converge to the values of unity and zero in the real and imaginary spectra indicating that the lower frequencies are less sensitive to differences in pulse shape.

CRITERION FOR PROXIMITY FAILURES

There are many types of equipment in which the change in distance between two elements due to the presence of a dynamic environment is a criterion for failure. A simple model of an equipment consisting of two mechanically uncoupled linear single-degree-of-freedom systems is shown schematically in Figure 33. The proximity of the two masses can change in accordance with dynamic excitations. If the distance between the masses becomes zero, collision occurs which may result in deformation or fracture of mechanical systems or direct shorts in electrical systems. The clearance between adjacent parts in mechanical systems may be either increased or decreased by the effects of an exciting motion. The results may lead to either malfunction or physical damage due to interaction of mechanical elements attributable to increased or decreased friction or interference between moving parts. In an electrical system, a multitude of failures can occur due to changes in the proximity of two elements. The direct result is a change of dielectric strength, magnetic or electrostatic field strengths. These in turn cause breakdowns in insulation, changes in capacitance, inductance, mutual inductance, etc., leading to any number of malfunctions or to permanent damage to components of the electrical system.

If a ground acceleration $\ddot{u}(t)$ is applied to the simple equipment of Figure 33, it causes a displacement of the base $u(t)$ which is transmitted to the two masses through the rigid frame and the springs and dampers of the equipment. The absolute motions of the adjacent surfaces of the two masses are $x_1(t)$ and $x_2(t)$. The relative displacements of these two masses are $\delta_1(t)$ and $\delta_2(t)$. The proximity of the masses at any time is the distance $D(t)$ and D_{st} is the static value when the system is at rest.

$$D(t) = x_2(t) - x_1(t) + D_{st}$$

$$x_1(t) = u(t) + \delta_1(t)$$

$$x_2(t) = u(t) + \delta_2(t)$$

Substituting for $x_1(t)$ and $x_2(t)$ in the first equation:

$$D(t) = \delta_2(t) - \delta_1(t) + D_{st} = \Delta(t) + D_{st}$$

The symbol D is called the "proximity" and Δ is called the "proximity criterion."

While the complete time history of the proximity function $D(t)$ might be enlightening, most engineers would find the extreme values more useful.

$$D_{\max} = D_{\text{st}} + \Delta_{\max}$$

$$D_{\min} = D_{\text{st}} + \Delta_{\min}$$

If the equipment is excited in both positive and negative directions, the maximum absolute value of the proximity function is of most importance.

$$|D|_{\max} = |D_{\text{st}} + \Delta|_{\max}$$

Thus Δ is established as an important criterion for determining the proximity failure potential of an exciting motion. This is somewhat analogous to the equivalent static acceleration of a single degree-of-freedom system which Walsh and Blake (Reference 26) proposed as a criterion for the failure potential of a motion. The latter is usually plotted as a positive function of the frequency of an undamped system and called the shock spectrum.

This suggests the possibility that "proximity spectra" might be determined by plotting Δ_{\max} and Δ_{\min} for the two-mass system of Figure 33. Since an additional mass is present, it would require a second frequency axis. Such a scheme would generate two surfaces (Δ_{\max} and Δ_{\min}) on a three dimensional plot. The development of this idea, however, is beyond the scope of this paper.

An upper bound for the proximity criterion Δ can be obtained from the undamped positive shock spectrum by adding the relative displacements. Δ_{\max} and $|\Delta|_{\max}$ would be the positive value of this sum and Δ_{\min} would be the negative value. This method provides a conservative estimate of the possibility of collision or proximity failures.

An indication of the possibility of overconservatism may be obtained by examining the undamped residual spectrum (or the undamped negative spectrum). If the proximity criterion has one or more extreme values in the residual era, that is, after the excitation has ceased, its positive and negative values may be much less than those determined from the positive spectrum. This is particularly true if the pulse tends toward symmetry. Since it cannot be determined whether the extremes of proximity occur during the pulse, after the pulse is over, or in both eras, when the negative (or residual) spectrum is different from the positive spectrum, it will be necessary to compute the time history of the proximity criterion if an over-conservative estimate is unacceptable.

The preceding discussion also applies to the determination of the proximity criterion for the model equipment with damped spring mass systems.

Although the proximity criterion has been developed for study of shock excitations there is no reason to limit it to shock. It can also be useful in the study of the proximity failure potential of random and multi-sinusoidal vibration and other forms of excitation.

SAWTOOTH VERSUS HALF-SINE

Another reason will be advanced in this section for preference of the terminal peak sawtooth for a general test. Two other reasons have already been discussed.

It has already been pointed out that the positive spectrum of the half-sine pulse is less constant than that of the sawtooth and there are nulls in the negative spectrum. In other words, the half-sine pulse shows much more frequency discrimination than the sawtooth. If it could be shown that the environment discriminated against these frequencies in the same way, one could say the half-sine would be an ideal test. Unfortunately, this is not so. The environment for a variety of equipments mounted in a variety of ways on a variety of structures in a variety of vehicles is largely unpredictable. The result is usually a somewhat arbitrary estimate of a positive and negative design shock spectrum of constant acceleration over a given frequency range. In other words, the design spectrum for a general test must be nondiscriminatory since we cannot predict how nature will discriminate against certain frequencies.

In the past, it has been assumed that if one were willing to overtest at some frequencies by as much as 76 percent, the half-sine would produce the minimum positive and negative values by testing in both positive and negative directions along the test axis of the equipment.

The half-sine pulses of military specifications were not based on shock spectra, but on expected acceleration inputs from the environment with no consideration of the spectral character of the environment.

There are several ways of judging the equivalence of the half-sine and sawtooth waves for comparison purposes. The method used here was to assume that the pulses were equivalent if they were equal in area and duration. This means that the peak amplitude of the sawtooth is $4/\pi$ times the peak amplitude of the half-sine. This is partially justified when it is realized that an environmental response spectrum based on half-sine inputs with various durations would be 1.76 times the input amplitude. The maximum response to the equivalent sawtooth is 1.61 times the input. The energy requirements for both pulses are equal.

Proximity criteria Δ for the model equipment of Figure 33 were computed on an analog computer for an ideal half-sine of unit amplitude and unit duration and an ideal sawtooth having an amplitude of $4/\pi$ and unit duration. The frequencies f_1 and f_2 were 1.5 and 1.55 respectively. These frequencies are in cycles per unit time. If the unit of time is 10 milliseconds, the pulses would be 10 milliseconds long and the response frequencies would be 150 and 155 cycles per second. They were chosen so that the residual responses were at or near a null in the residual spectrum and were also close together. The first of these conditions insures that the residual responses will be at or near zero. The second condition would insure that the two responses would be very nearly in phase with each other during the excitation, and the proximity criterion in this case would also be nearly zero. This is shown to be true by examination of the first computer record from the left of Figure 34. Positive, negative, and absolute values of the proximity criterion are all very small in comparison to the proximity criteria for the sawtooth shown in the second record. The third and fourth records compare the proximity criteria when a goodly amount of damping ($\zeta = 0.1$) is present. These proximity criteria cannot be compared directly to those in the first and second records, because the amplitude scale is different. They are actually smaller than those for the undamped cases. It is seen that the

addition of damping greatly reduces the proximity criterion in the residual eras, but has much less effect on those during the excitation era. Nevertheless, the sawtooth still produces larger values of positive, negative, and absolute proximity criteria.

The same equipment was also subjected to pulses having a relative duration of .4333 as shown in Figure 35. This pulse length was chosen to nearly maximize extreme values of the proximity criteria for the half-sine excitation. The same results would have been obtained if the duration had remained at unity and the frequencies of the two systems had been changed by the factor .4333 to .65 and .672. A change in the input is analogous to a change in the environment while a change in the response frequencies is analogous to a change of an equipment being tested. It is evident that even near frequencies of maximum values for the positive, negative, and absolute proximity criteria of the half-sine, the proximity criteria of the sawtooth are 96 percent of those for the half-sine. It can be shown that a sawtooth pulse which produces the same maximum response at the same frequency as the half-sine and has the same area will produce the same extremes of the proximity criterion. This is another pulse which can be considered equivalent. This criterion for equivalence was actually used in converting Air Force half-sine tests to sawtooth tests.

CONCLUSIONS

(1) The ramp-sine function is more closely related to the actual test waveform generated during a sawtooth test than previous theoretical pulses and is more justifiable by physical reasoning.

(2) Shock spectra and Fourier spectra for a variety of deviations from ideal half-sine and sawtooth pulses have been determined. These spectra can be used in design work and in choosing test waveforms.

(3) The proximity criterion Δ proposed in this paper provides insight into the ability of a shock excitation to produce proximity or collision failures in a simple equipment which cannot be obtained from the shock spectrum. It can also be used to study other forms of excitation such as random vibration.

(4) On the basis of present knowledge, the terminal peak sawtooth is a considerably better waveform than the half-sine for creating proximity and collision failures in a simple equipment. This conclusion applies whether the test is applied in only one direction or in opposite directions along the test axis. Since the terminal peak sawtooth and half-sine are representative of the effects of asymmetry and symmetry, the conclusion can be generalized to show the superiority of asymmetrical over symmetrical waveforms.

(5) The effects of damping and drop-off time in the sawtooth pulse reduce the negative spectrum enough to warrant testing in both directions along each of the three principal axes. For example, damping and drop-off reduced the undamped negative response to an ideal pulse by 75 percent for a comparable 1000 cps system with 10 percent damping. (This does not mean that the negative spectrum is unimportant. It is quite important when proximity failures are considered.)

(6) Negative spectra should be plotted as part of any data reduction process which results in shock response spectra since this spectrum is important in assessing the possibility of proximity failures.

REFERENCES

1. Morrow, C. T., and H. I. Sargeant. "Sawtooth Shock as a Component Test." Acoust. Soc. Am 28:959 (1956).
2. Lowe, R., and R. D. Cavanaugh. "Correlation of Shock Spectra and Pulse Shape with Shock Environment." Environmental Engineering, Vol. 1, No. 1. Feb 1959.
3. Vigness, I., and E. W. Clements. Sawtooth and Half-Sine Shock Impulses from the Navy Shock Machine for Medium Weight Equipment. NRL Report 5934, Naval Research Laboratory, Washington (1963).
4. Morrow, C. T. Shock and Vibration Engineering, Vol. 1. John Wiley and Sons, New York (1963).
5. Jacobsen, L. S., and R. S. Ayre. Engineering Vibrations. McGraw-Hill Book Co., Inc., New York (1958), Ch. 4, et al.
6. Harris, C. M., and C. E. Crede (Editors). Shock and Vibration Handbook. McGraw-Hill Book Co., Inc., New York, Ch. 8, Ch. 23 (1961).
7. Luk, R. R. The Impact Response of a Single-Degree-of-Freedom System with Viscous Damping. Structural Mechanics Research Laboratory, The University of Texas (1960).
8. Molloy, C. T. "Use of Four-Pole Parameters in Vibration Calculations." Journal of the Acoustical Society of America, 29:842 (1957).
9. Mains, R. M. "Structural Response to Dynamic Load," Shock, Vibration and Associated Environments. Bul. 30, Part II: 66, Naval Research Laboratory, Washington (1962).
10. Painter, G. W., and H. J. Parry. "Simulating Flight Environment Shock on an Electrodynamical Shaker." Shock, Vibration, and Associated Environments. Bul. 33, Part III: 85, Naval Research Laboratory, Washington (1964).
11. Discussion MEMO of MIL-STD-810 Dynamics Conference, Flight Dynamics Laboratory, Wright-Patterson AFB, Ohio (1962).
12. Morrow, C. T., "Reflections on Shock and Vibration Technology." Shock, Vibration and Associated Environments, Bul. 33, Part II: 8, Naval Research Laboratory, Washington (1964).
13. Crede, C. E. Vibration and Shock Isolation. John Wiley and Sons, Inc., New York (1951).
14. Thomson, W. T. Mechanical Vibrations. Prentice-Hall Inc., Englewood Cliffs, N. J. (1953).

REFERENCES (Continued)

15. Crandall, S. H., et al. Random Vibration, Vol. I. The M.I.T. Press, Cambridge, Mass. (1958).
16. Den Hartog, J. P. Mechanical Vibrations, 4th ed. McGraw-Hill Book Co., Inc. New York (1956).
17. von Karman, T., and M. A. Biot. Mathematical Methods in Engineering. McGraw-Hill Book Co., Inc., New York (1940).
18. Wylie, C. R., Jr. Advanced Engineering Mathematics. McGraw-Hill Book Co., Inc., New York (1960).
19. Brooks, R. O. "The Use of Graphical Techniques to Analyze Shock Motions of Lightly Damped Linear Spring Mass Systems." Shock, Vibration, and Associated Environments, Bul. 33, Part II:195, Naval Research Lab. Washington (1964).
20. Biot, M. A. "A Mechanical Analyzer for the Prediction of Earthquake Stresses." Bul. of the Seismological Society of America, V.31:143, Apr 1941.
21. Biot, M. A. "Analytical and Experimental Methods in Engineering Seismology." Trans of the American Society of Civil Engineers, 108:365 (1943).
22. Fung, Y. C., and M. V. Barton. "Some Shock Spectra Characteristics and Uses." Journal of Applied Mechanics V.25:365, Sep 1958.
23. Rubin, S. "Response of Complex Structures from Reed Gage Data." Journal of Applied Mechanics, 25:501, Dec 1958.
24. Marous, J. J., and E. H. Schell. "An Analog Computer Technique for Obtaining Shock Spectra." Shock, Vibration, and Associated Environments, Bul. 33, Part II: 182 (1964).
25. Shapiro, H., and D. E. Hudson. "The Measurement of Acceleration Pulses with the Multi-Frequency Reed Gage." Journal of Applied Mechanics, V.20:422, Sept 1953.
26. Walsh, J. P. and R. E. Blake. The Equivalent Static Acceleration of Shock Motions. NRL Report F-3302, Naval Research Laboratory, Washington (1948).

APPENDIX

FORMULAS AND TABLES

Point of Tangency of the Ramp-Sine Function

The point of tangency of the ramp-sine function (B, T_1) is determined from the condition that both $f_1(t)$ and $f_2(t)$ are equal at time T_1 and their slopes are also equal at T_1 . These conditions lead to the following pair of simultaneous equations:

$$B - A \sin \frac{\pi(T_1 - 2T_R + T)}{2(T - T_R)} = 0$$

$$\frac{B}{T_1} - \frac{\pi A}{2(T - T_R)} \cos \frac{\pi(T_1 - 2T_R + T)}{2(T - T_R)} = 0$$

The solution of this pair is:

$$T_1 = \frac{2(T - T_R)}{\pi} \tan \frac{\pi(T_1 - 2T_R + T)}{2(T - T_R)}$$

This is a transcendental equation and an exact analytical solution cannot be obtained. It was evaluated by iterative methods on a digital computer. B was then evaluated by substituting T_1 in the first of the simultaneous pair. The evaluations of B and T_1 were carried out for various ratios of T_R/T . The normalized results of these computations are compiled in Table 1. Values of B and T_1 for values of T_R/T not listed may be interpolated. B and T_1 may be obtained from the table value by multiplying by A and T respectively.

Determination of Area of Ramp-Sine Function

The determination of the value of $F(0)$ for normalization of the Fourier spectra is as follows:

$$F(\omega) = \int_0^T f(t) e^{-j\omega t} dt$$

When $\omega = 0$, this reduces to:

$$F(0) = \int_0^T f(t) dt$$

This is simply the area between the excitation function and the time axis.

For the ramp-sine function:

$$F(t) = \frac{B}{T_1} \int_0^{T_1} t dt + A \int_{T_1}^T \sin \frac{\pi(t - 2T_R + T)}{2(T - T_R)} dt$$

the solution of this equation is:

$$F(t) = \frac{BT_1}{2} + \frac{2A(T - T_R)}{\pi} \left[\cos \frac{\pi(T - 2T_R)}{2(T - T_R)} \left(\cos \frac{\pi T_1}{2(T - T_R)} - \cos \frac{\pi T}{2(T - T_R)} \right) \right. \\ \left. + \sin \frac{\pi(T - 2T_R)}{2(T - T_R)} \left(\sin \frac{\pi T}{2(T - T_R)} - \sin \frac{\pi T_1}{2(T - T_R)} \right) \right]$$

This equation has been solved for a number of T_R/T ratios. The values computed have been normalized by division by the product AT . They are included in Table 1.

Alternate Excitations and Responses

Several alternate forms of excitation and responses are given in Tables 2 and 3. In general an excitation which is the n th derivative or integral of any excitation in the tables results in a response which is the n th derivative or integral of the corresponding tabular response.

TABLE 1

FREQUENCY AND AREA* DATA FOR THE RAMP-SINE FUNCTION

T_R/T	B/A	T_I/T	F(0)/AT
1.0000	1.0000	1.0000	.500
.9756	.9999	.9754	.503
.9524	.9995	.9514	.507
.9302	.9989	.9281	.510
.9091	.9980	.9054	.513
.8889	.9968	.8832	.517
.8696	.9954	.8615	.520
.8511	.9937	.8404	.523
.8333	.9917	.8196	.526
.8065	.9880	.7873	.531
.7813	.9835	.7559	.536
.7576	.9781	.7252	.541
.7353	.9719	.6952	.546
.7143	.9647	.6658	.551
.6897	.9541	.6296	.557
.6667	.9417	.5938	.563
.6452	.9270	.5583	.569
.6250	.9096	.5227	.575
.6061	.8889	.4867	.581
.5882	.8641	.4500	.588
.5714	.8336	.4118	.595
.5556	.7955	.3713	.602
.5405	.7455	.3272	.609
.5263	.6756	.2763	.617
.5128	.5621	.2108	.625
.5000	.0000	.0000	.637

*F(0) is numerically equal to the area of the function.

TABLE 2

ALTERNATE FORMS OF EXCITATION AND UNDAMPED RESPONSE

Excitation (E)		Response (R)	
Force applied to mass (Ground immobile)	$\frac{F(t)}{k}$	Absolute displacement	x
Ground displacement	$u(t)$	Absolute displacement	x
Ground acceleration	$\frac{-\ddot{u}(t)}{\omega_n^2}$	Relative displacement	δ
Ground acceleration	$\ddot{u}(t)$	Absolute acceleration	\ddot{x}
Ground velocity	$\dot{u}(t)$	Absolute velocity	\dot{x}
nth derivative of ground displacement	$\frac{d^n u(t)}{dt^n}$	nth derivative of absolute displacement	$\frac{d^n x}{dt^n}$

TABLE 3

ALTERNATE FORMS OF EXCITATION AND DAMPED RESPONSE

Excitation (E)		Response (R)	
Force applied to mass (Ground immobile)	$\frac{F(t)}{k}$	Absolute displacement	x
Ground acceleration	$\frac{-\ddot{u}(t)}{\omega_n^2}$	Relative displacement	δ
Ground acceleration	$\ddot{u}(t)$	Relative displacement	$-\omega_n^2 \delta$

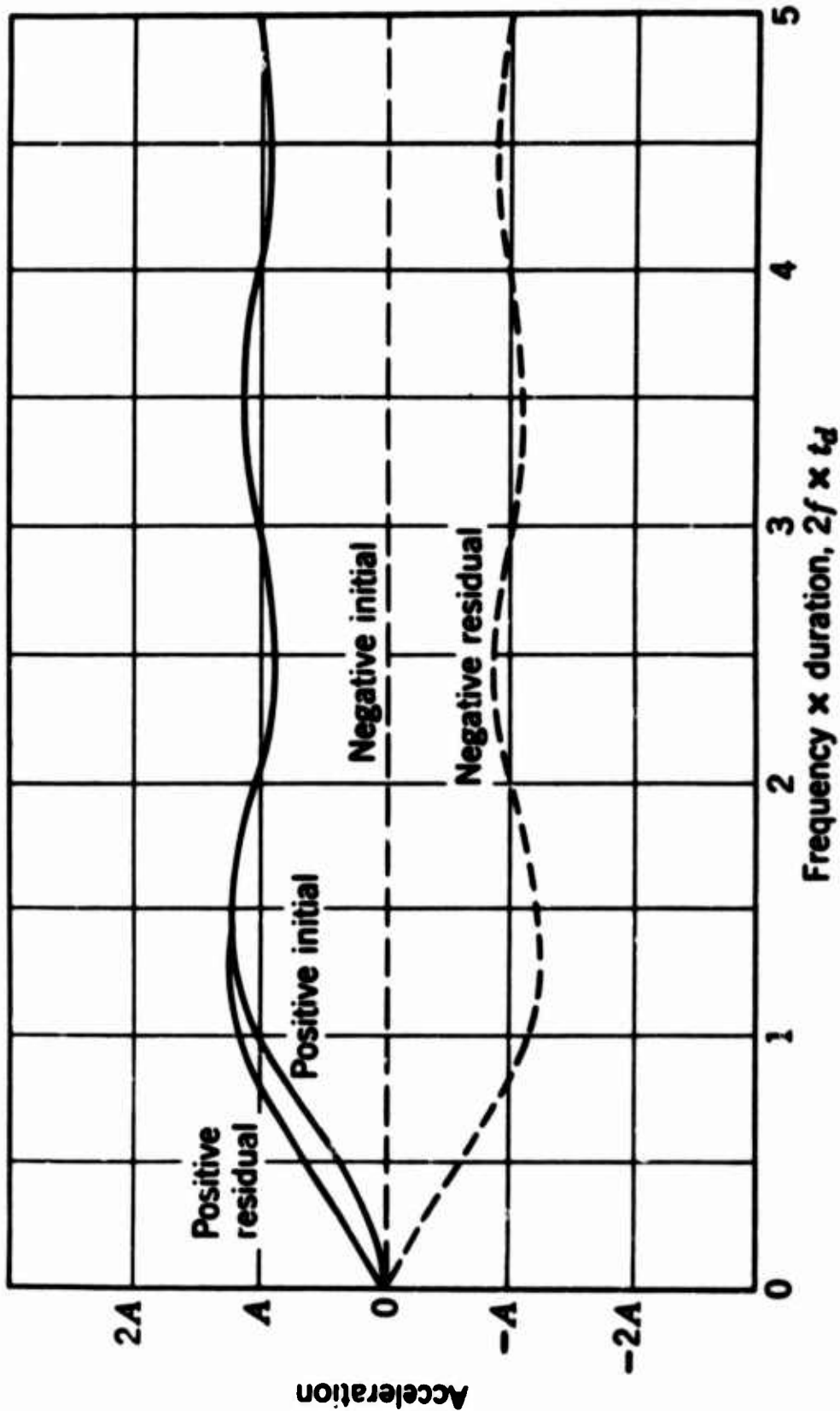


Figure 1. Ideal Sawtooth Spectra (After Morrow, Reference 4)

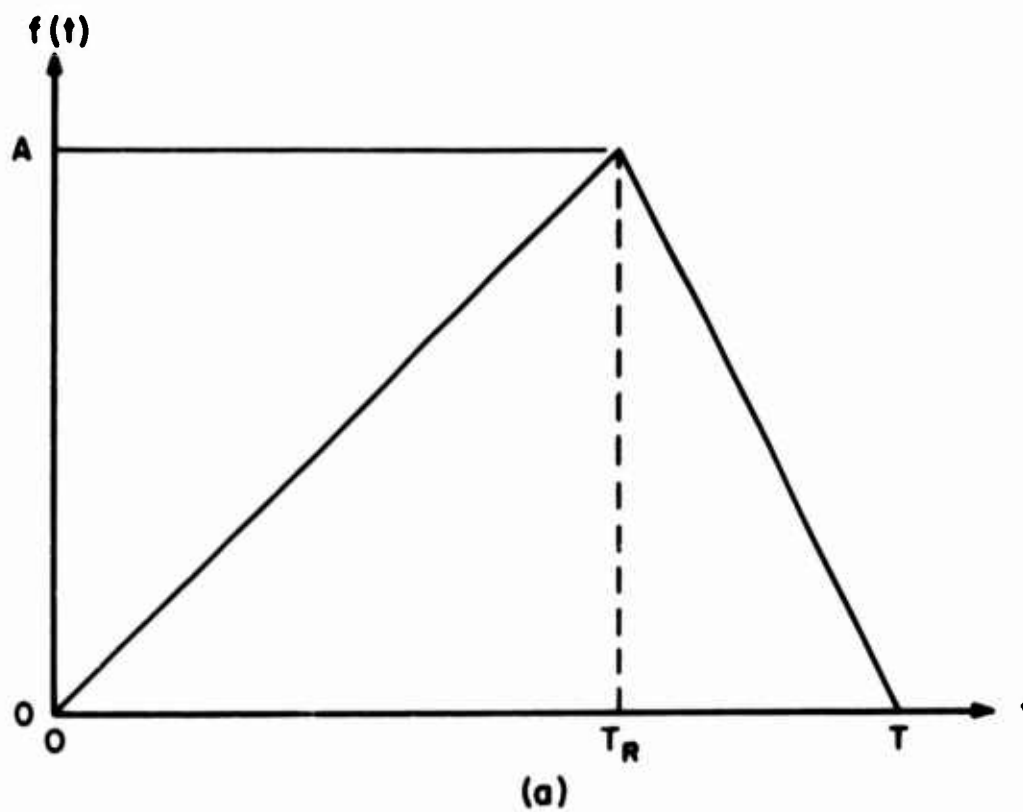


Figure 2. (a) Triangular Function Used in Previous Studies

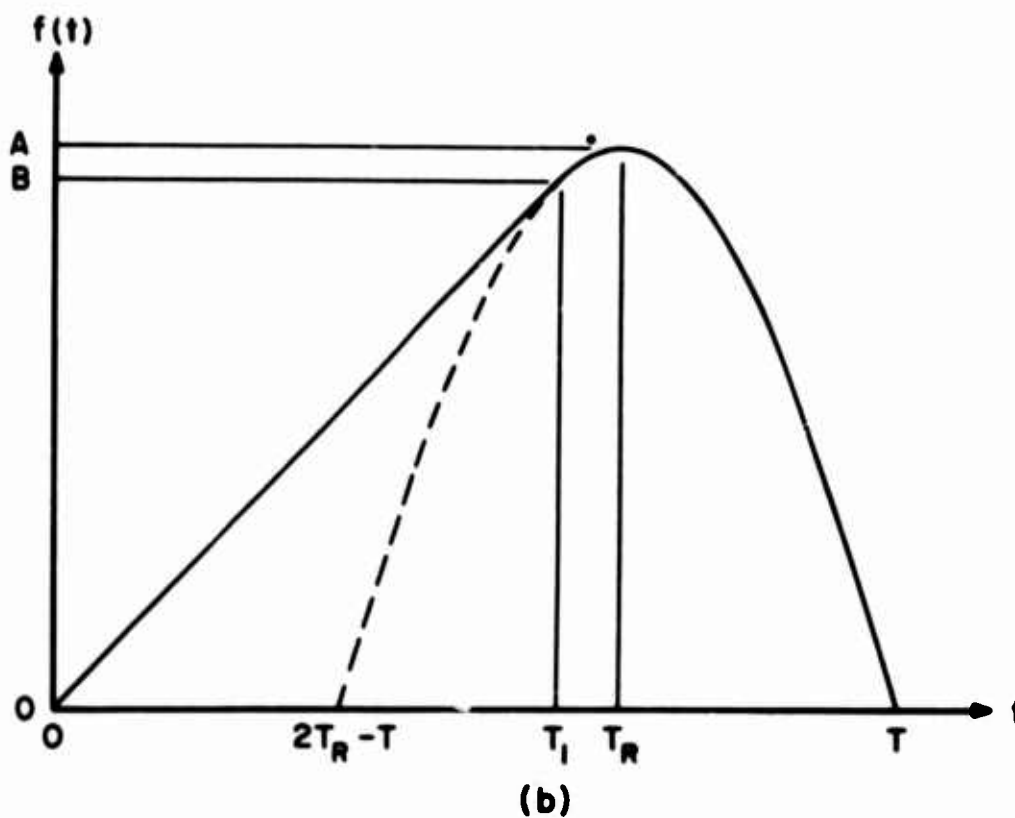


Figure 2. (b) Ramp-Sine Function Studied in This Report

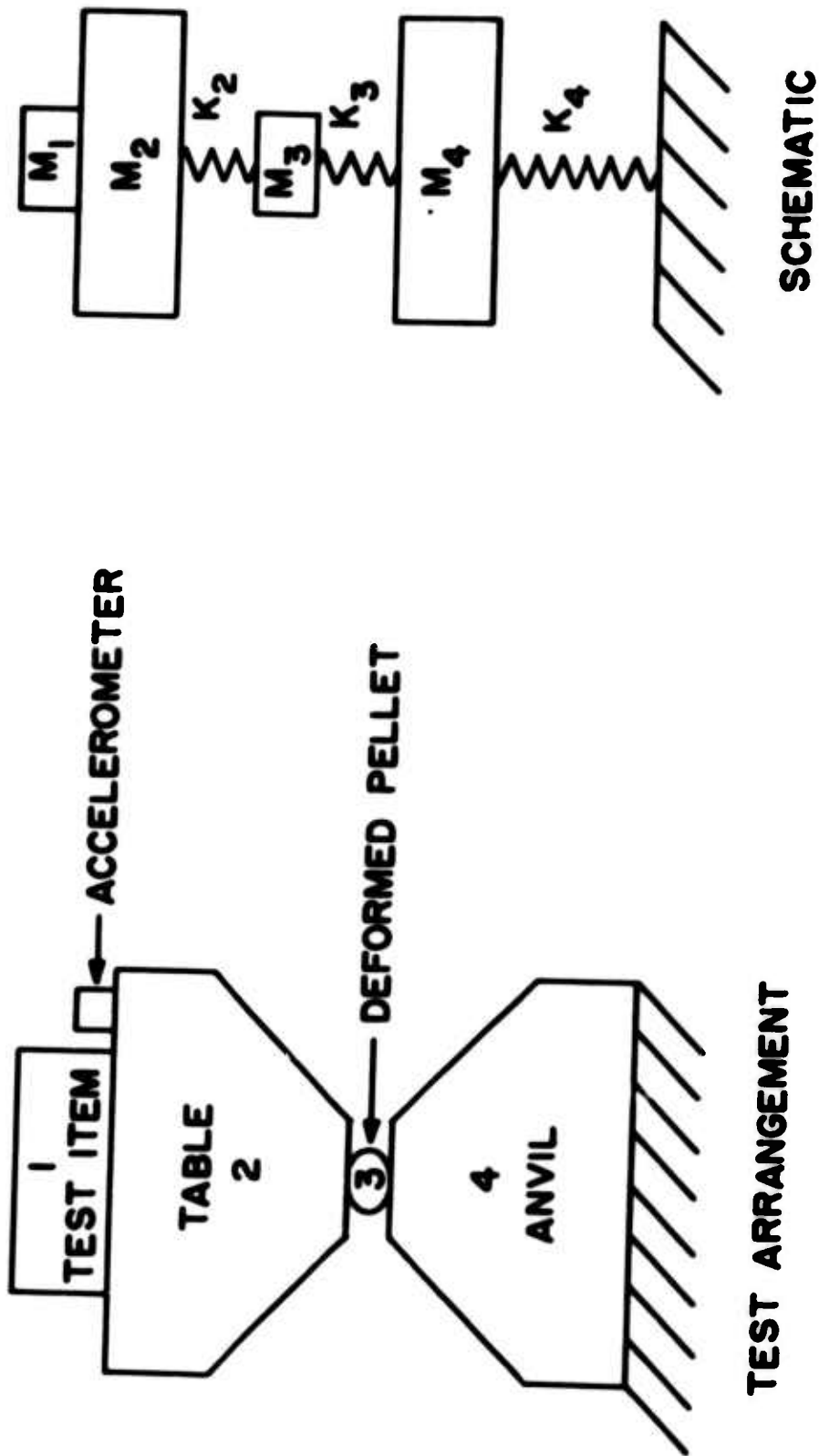


Figure 3. Test Setup and Schematic Representation

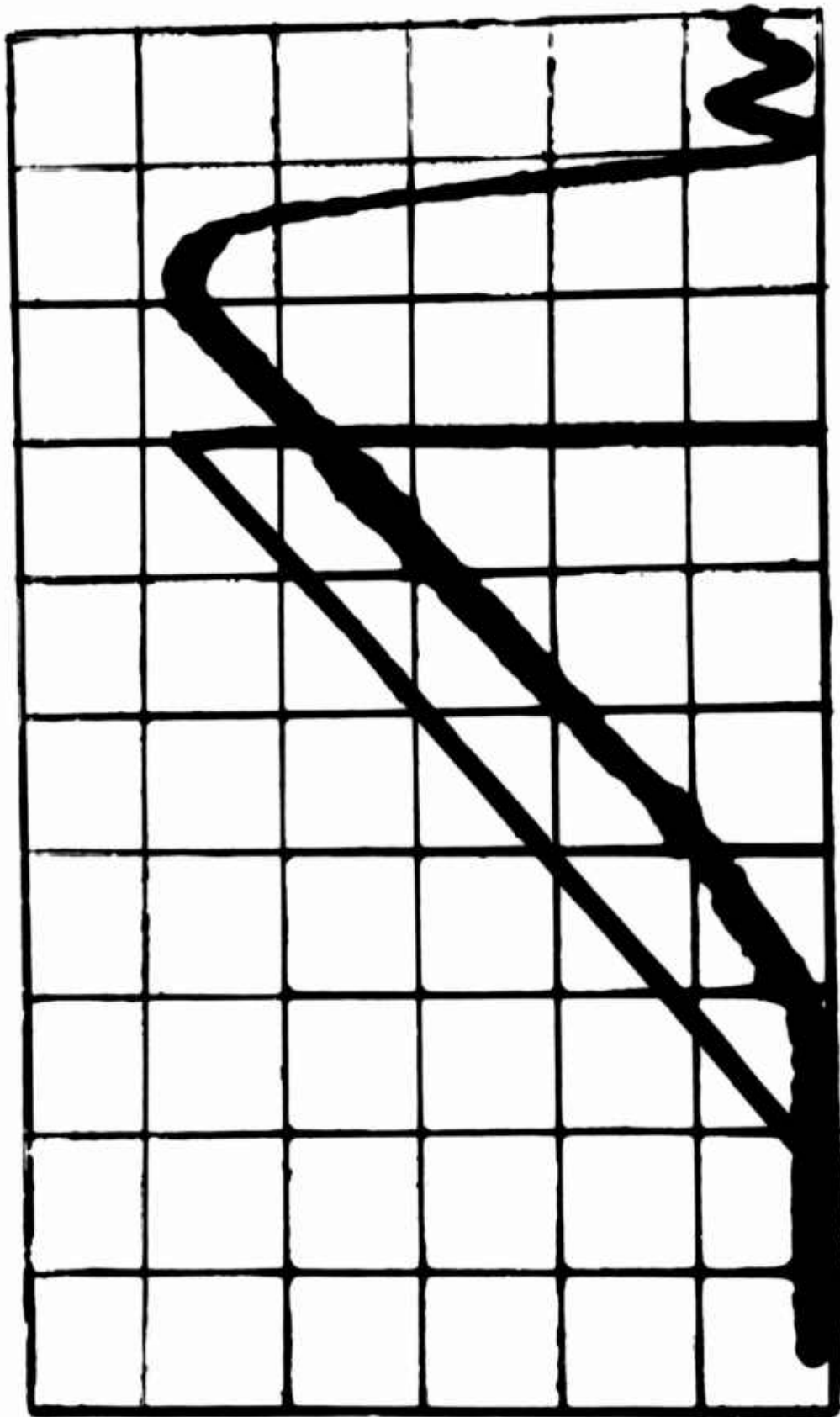


Figure 4. Comparison of a Record of an Actual Test Pulse With an Ideal Terminal Peak Sawtooth Pulse

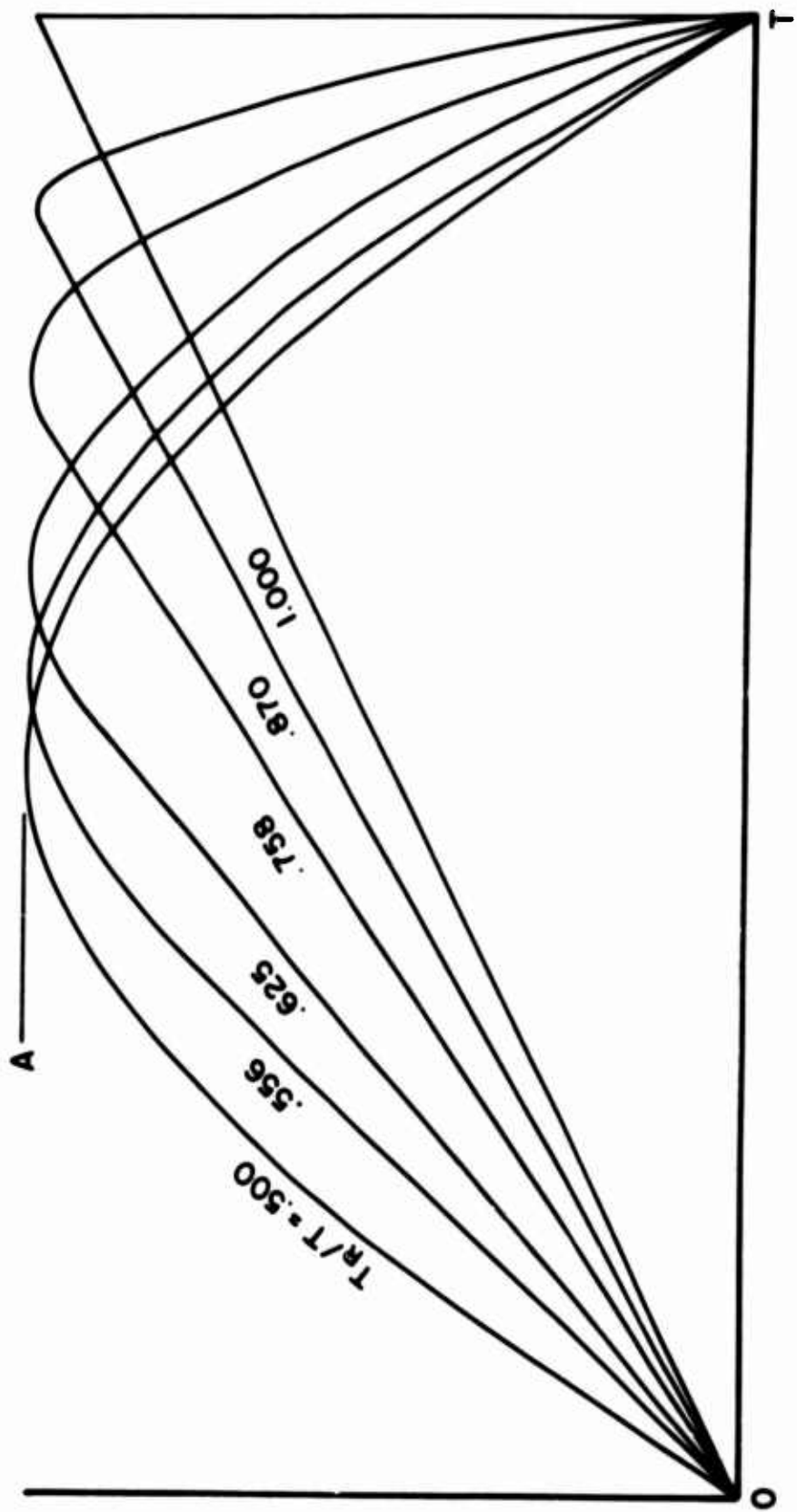


Figure 5. Ramp-Sine Pulses

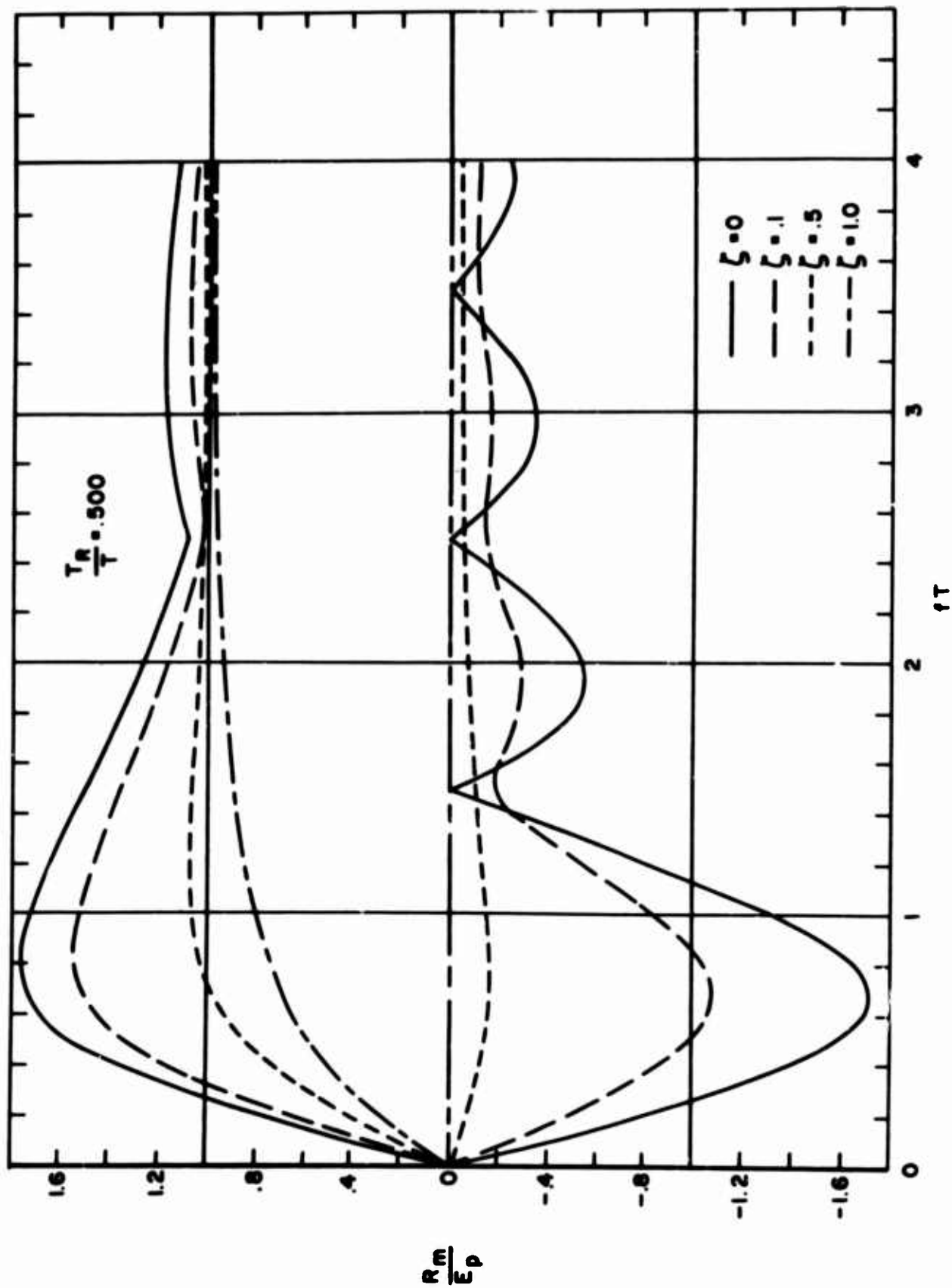


Figure 6. Half-Sine Response Spectra for $T_R/T = .5$

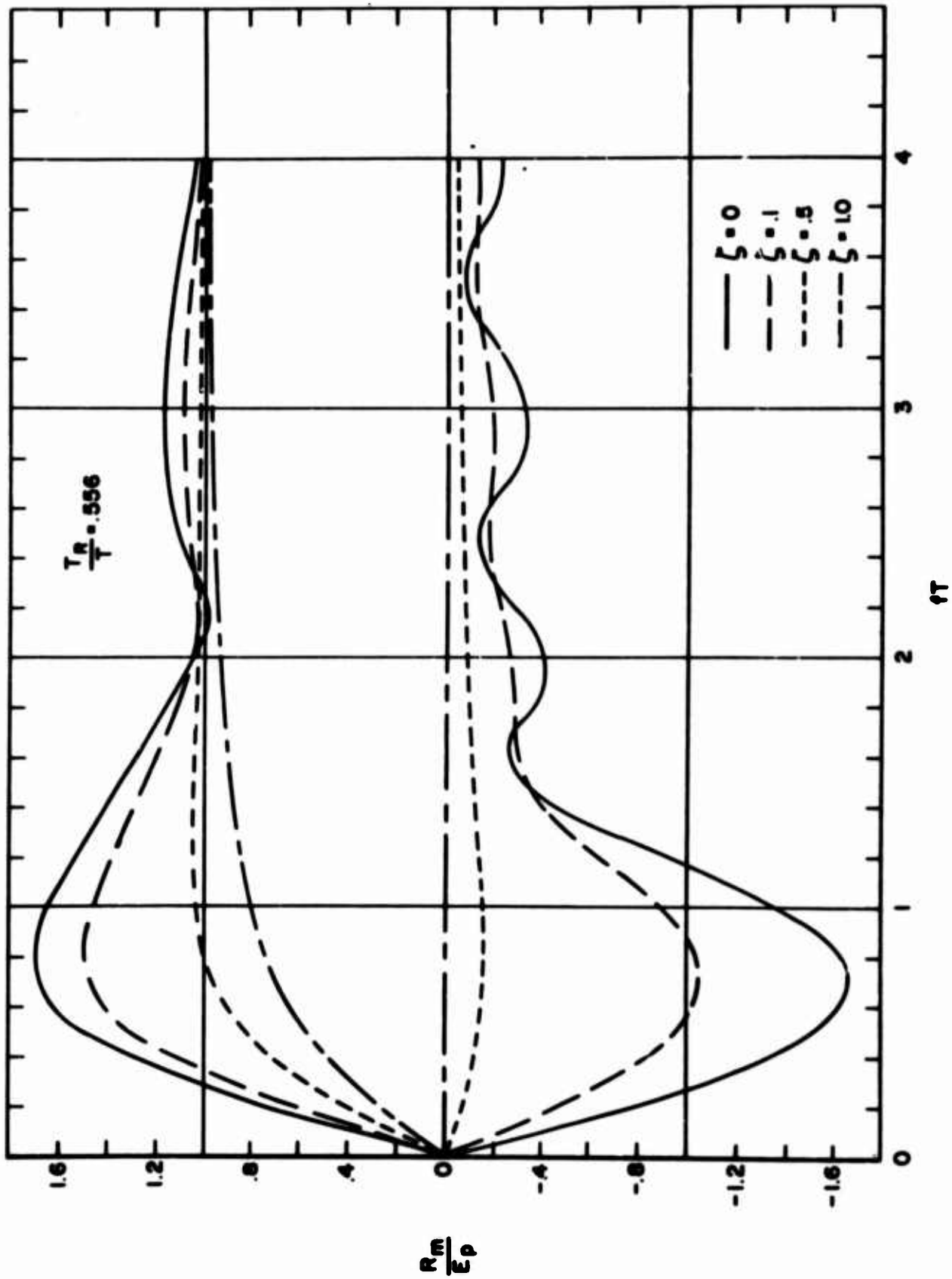


Figure 7. Ramp-Sine Response Spectra $T_R/T = .556$

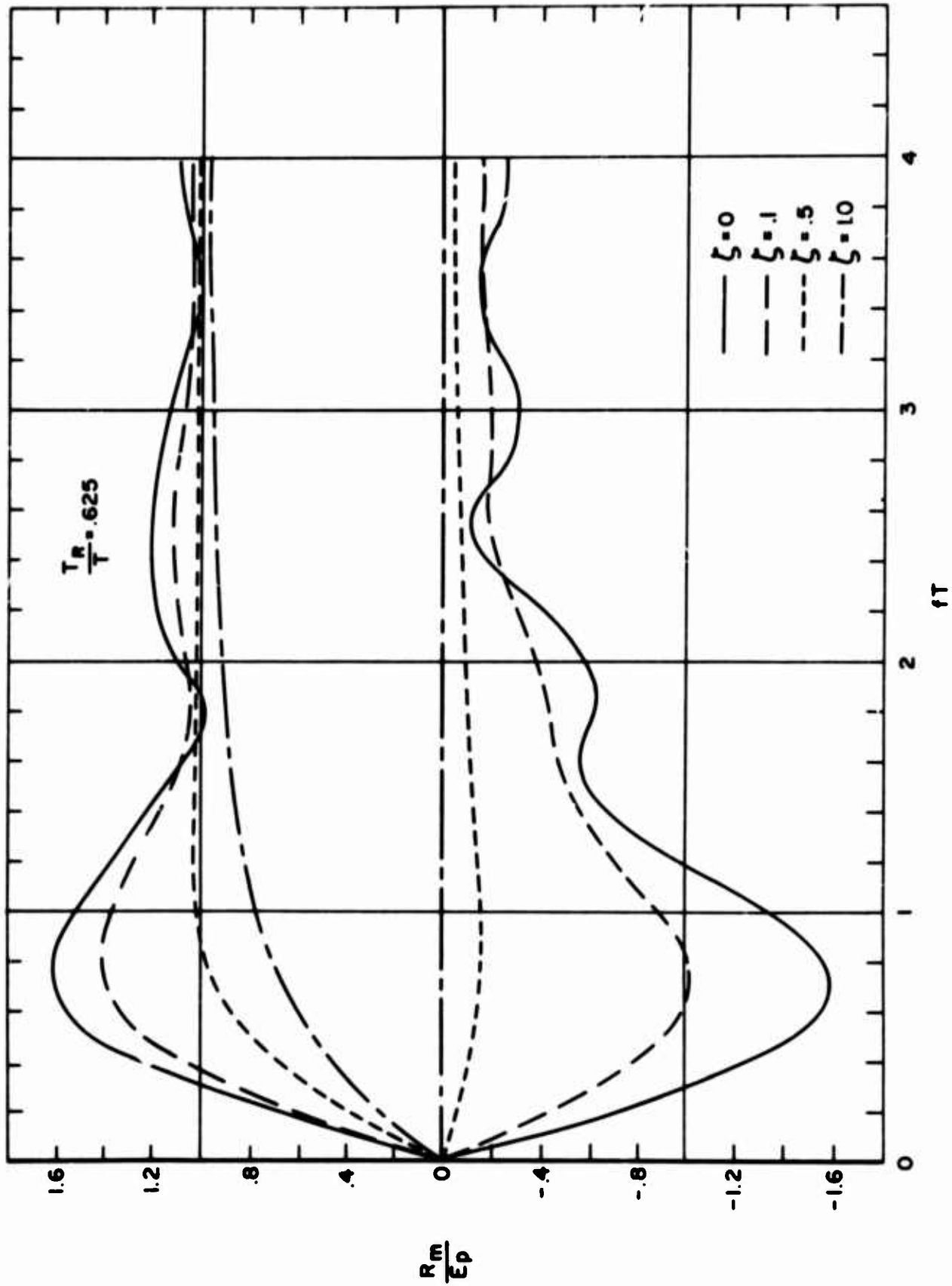


Figure 8. Ramp-Sine Response Spectra for $T_R/T = .625$

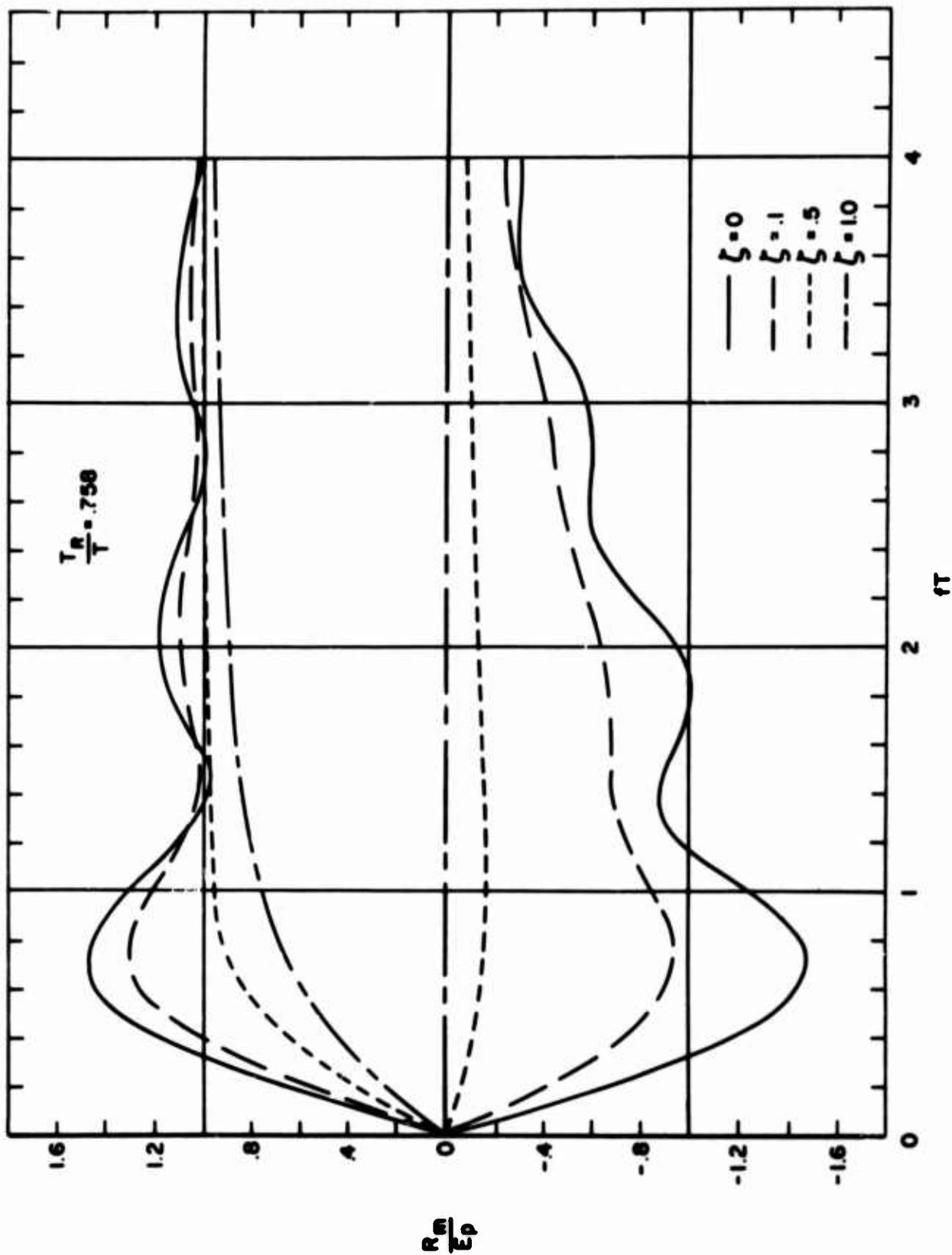


Figure 9. Ramp-Sine Response Spectra for $T_R/T = .758$

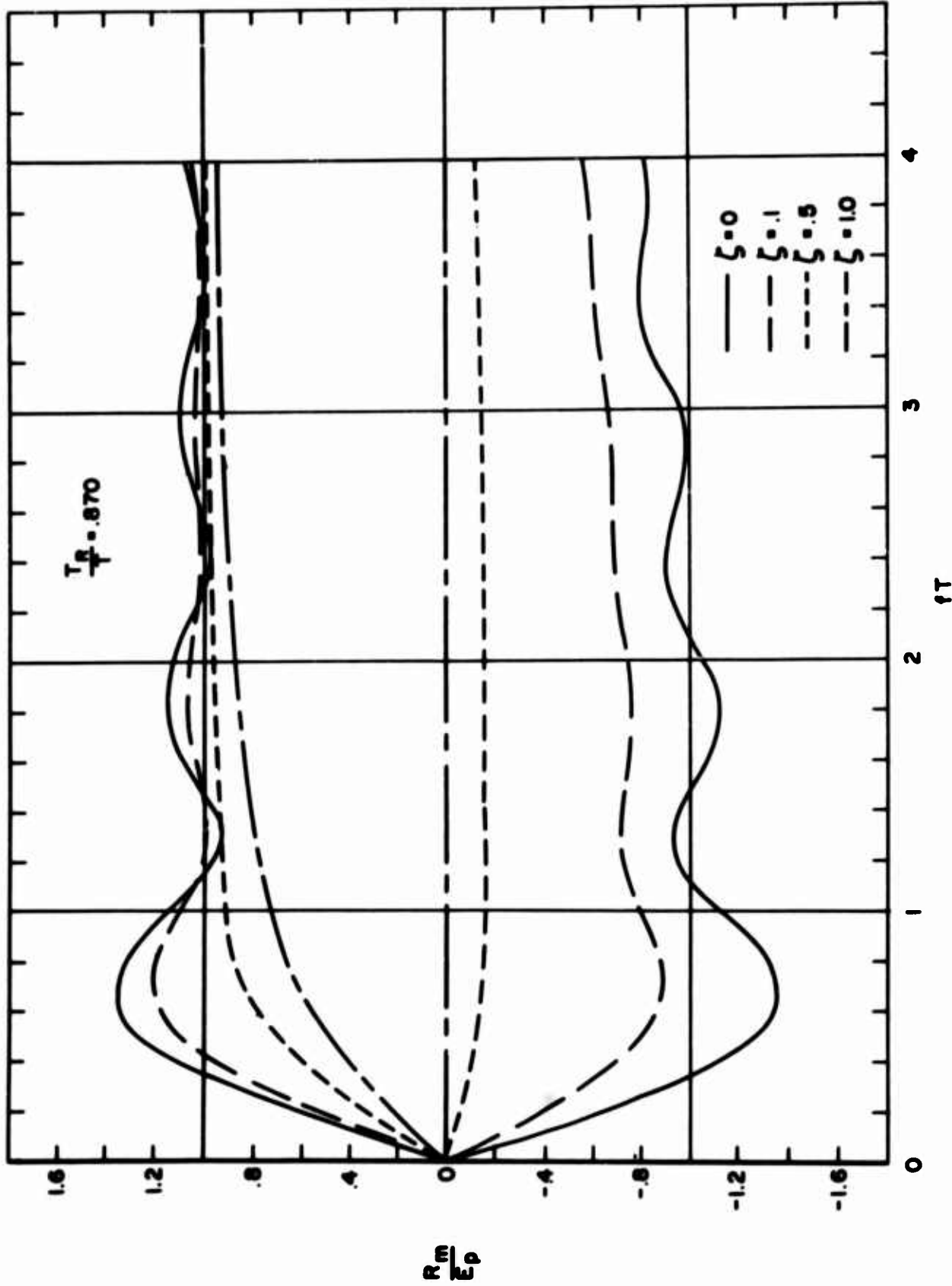


Figure 10. Ramp-Sine Response Spectra for $T_R/T = .870$

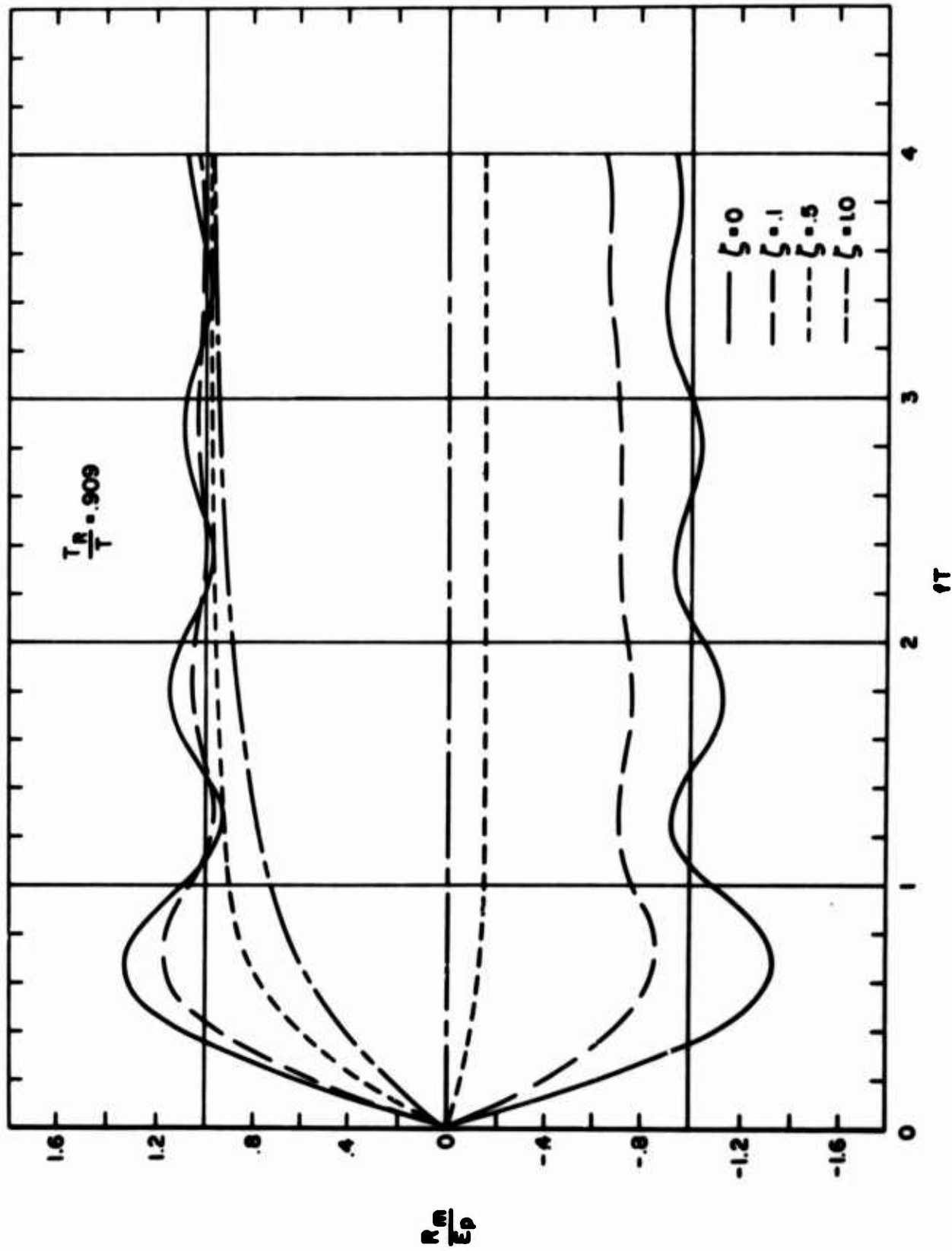


Figure 11. Ramp-Sine Response Spectra for $T_R/T = .909$

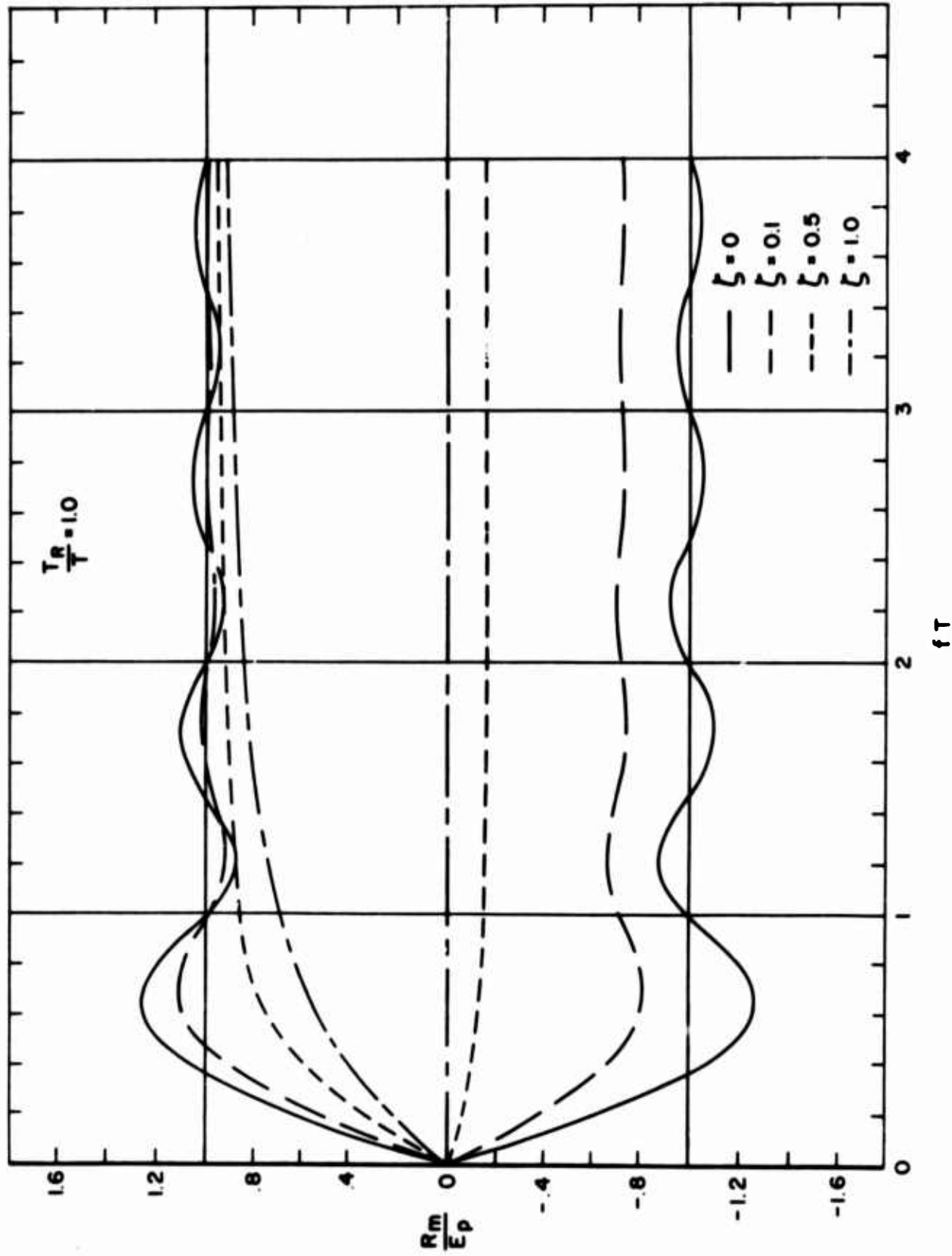


Figure 12. Ramp-Sine Response Spectra for $T_R/T = 1.000$

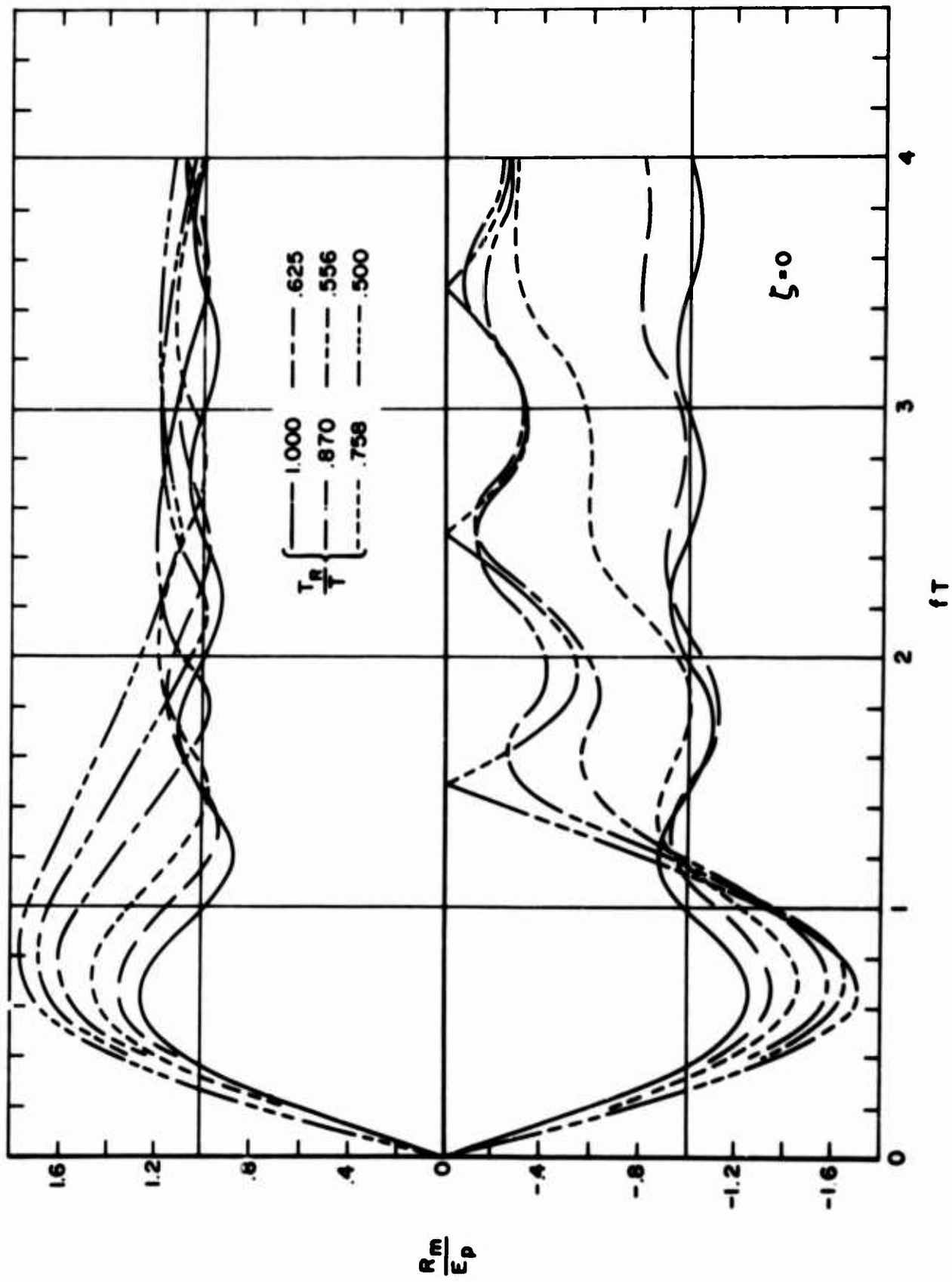


Figure 13. Variations in Response Spectra for $\zeta = 0$

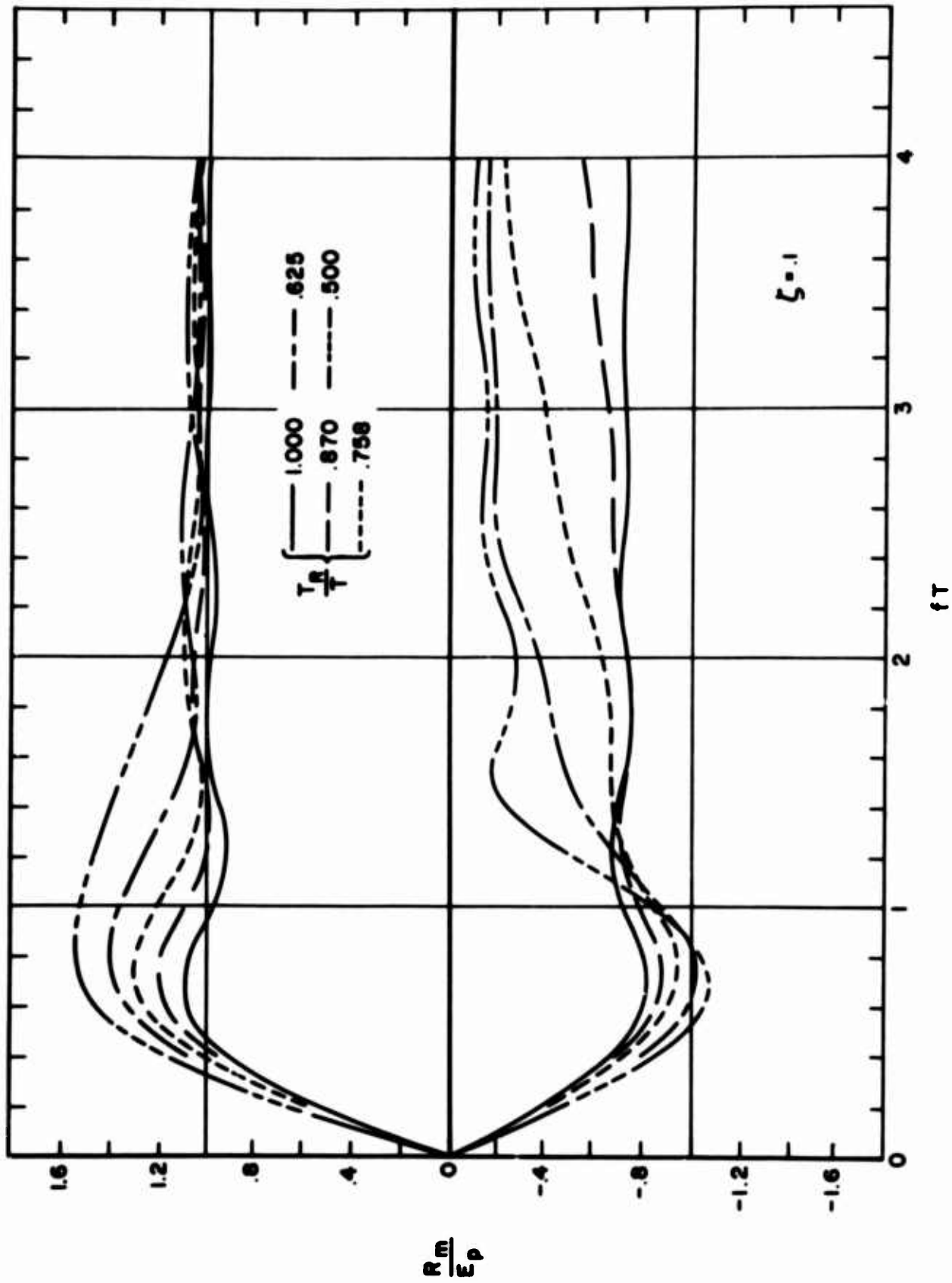


Figure 14. Variations in Response Spectra for $\zeta = 0.1$

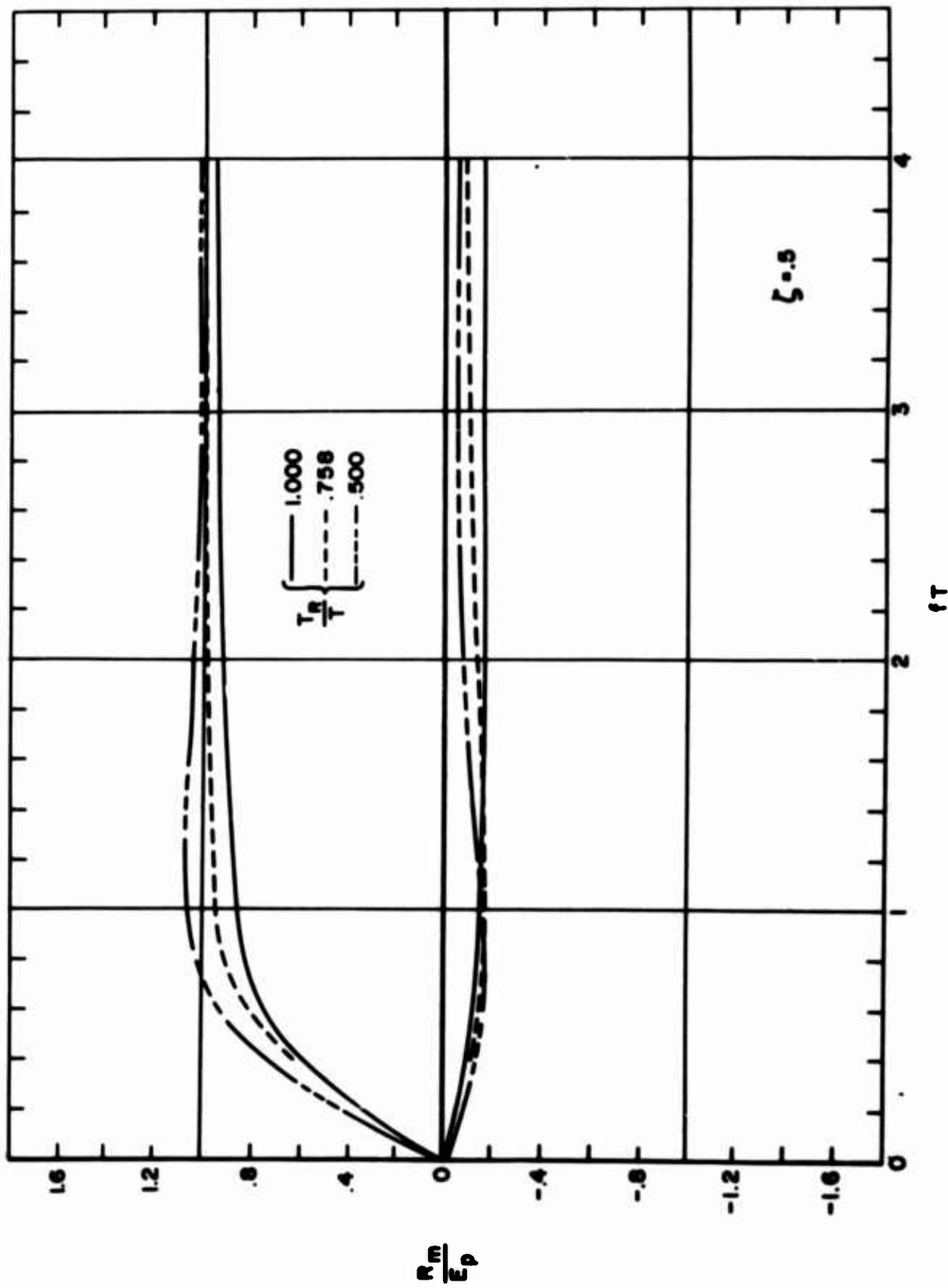


Figure 15. Variations in Response Spectra for $\zeta = 0.5$

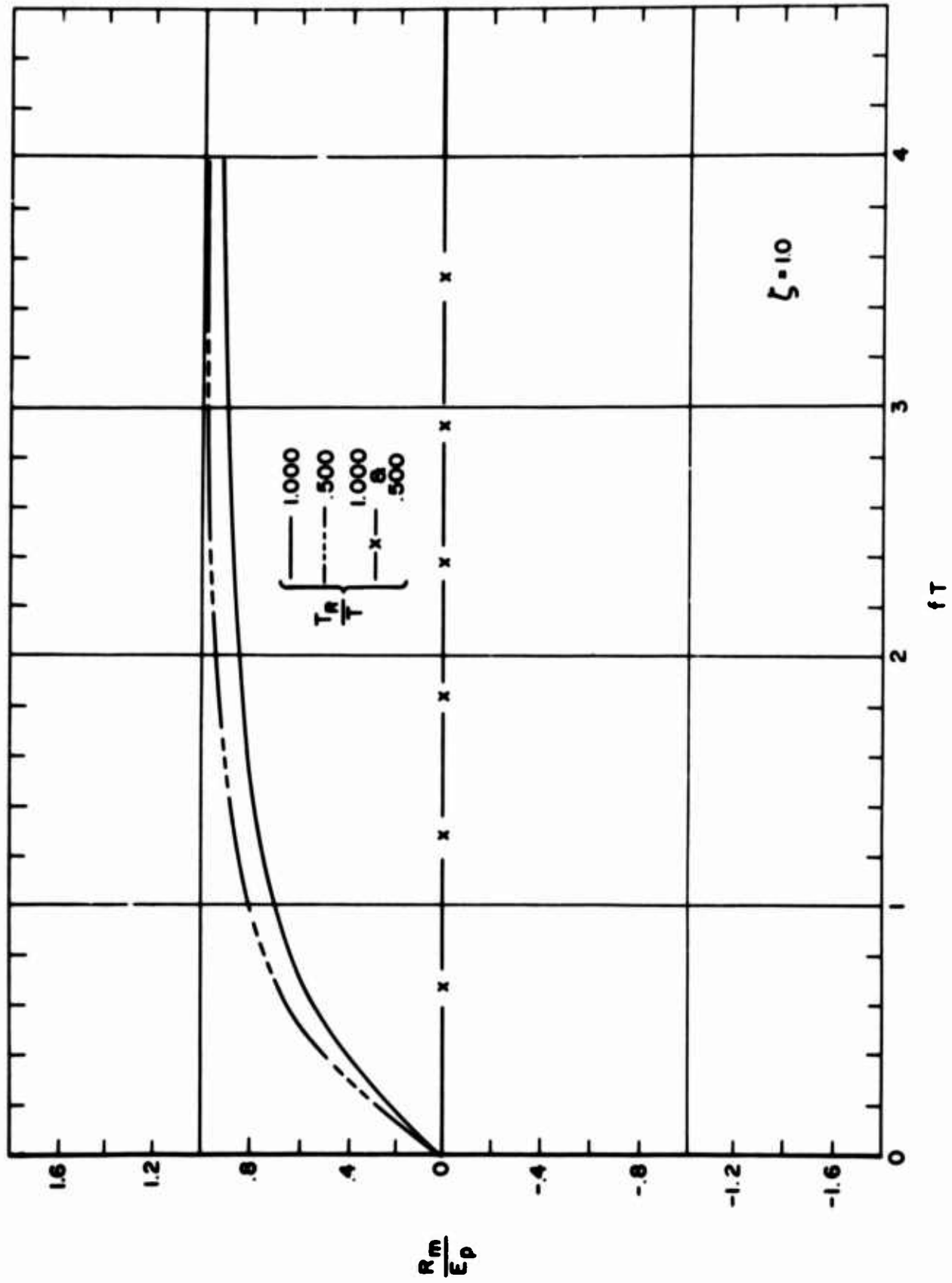


Figure 16. Variations in Response Spectra for $\zeta = 1.0$

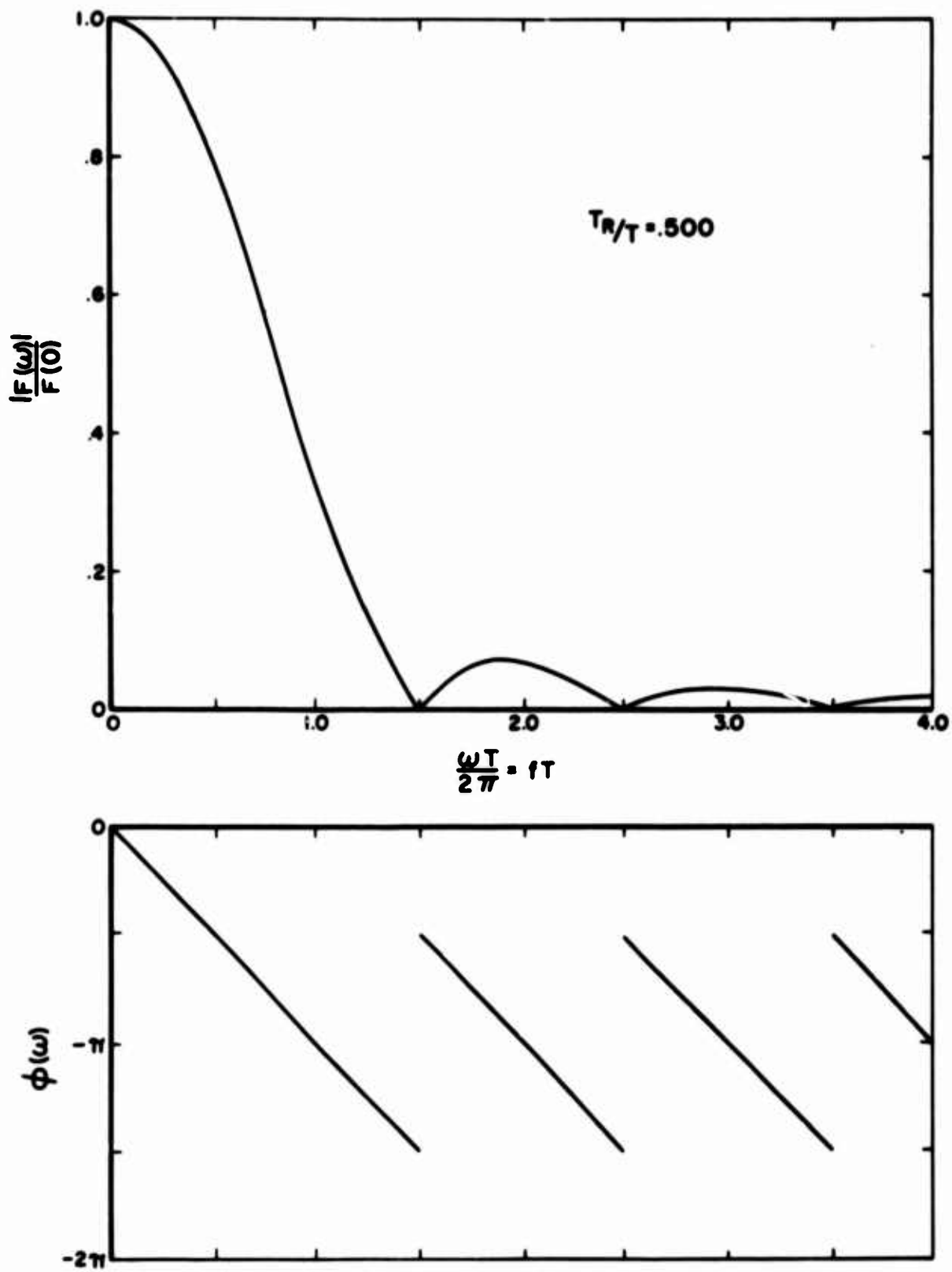


Figure 17. Fourier Amplitude and Phase Spectra for $T_R/T = .500$

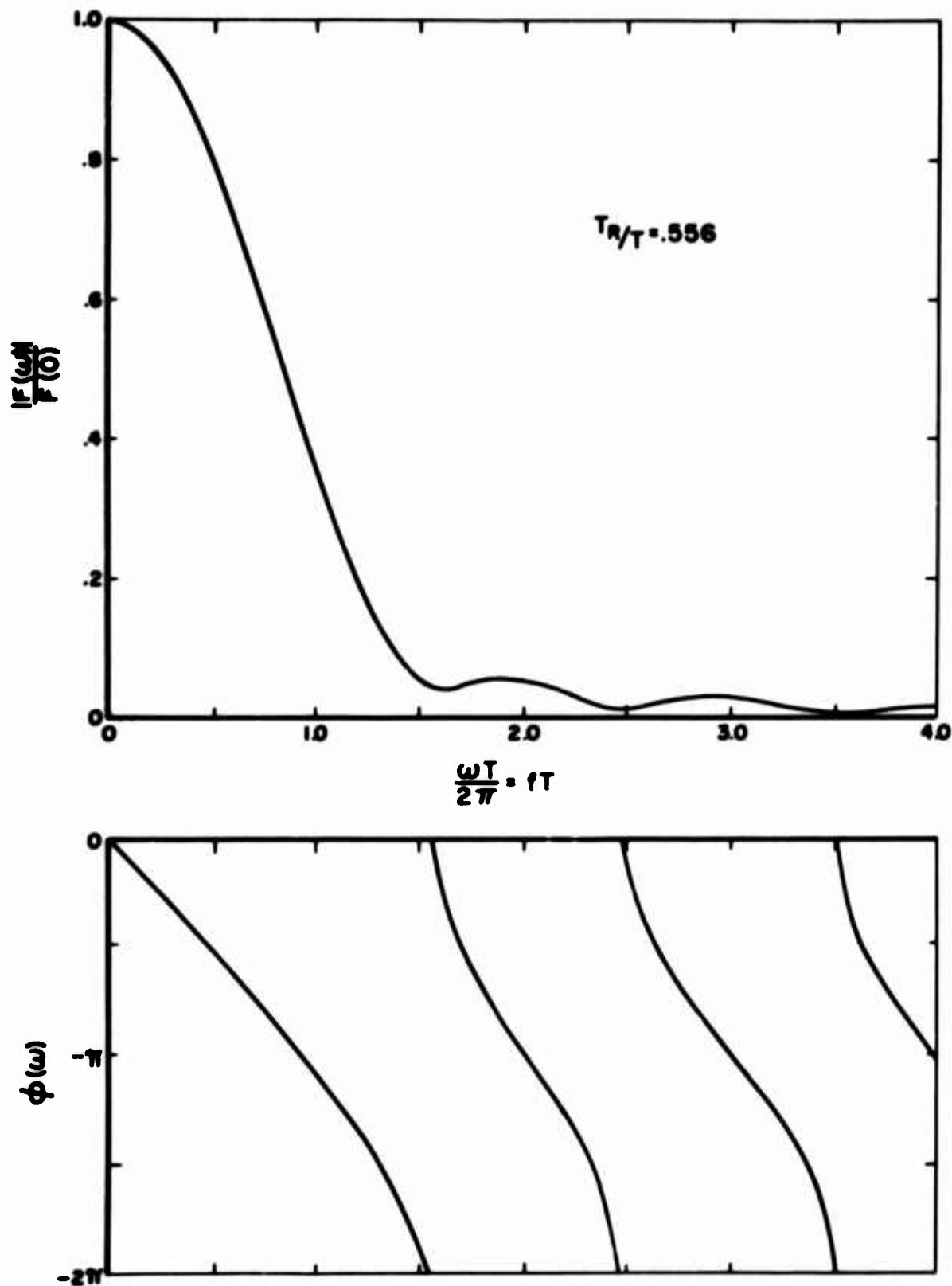


Figure 18. Fourier Amplitude and Phase Spectra for $T_R/T = .556$

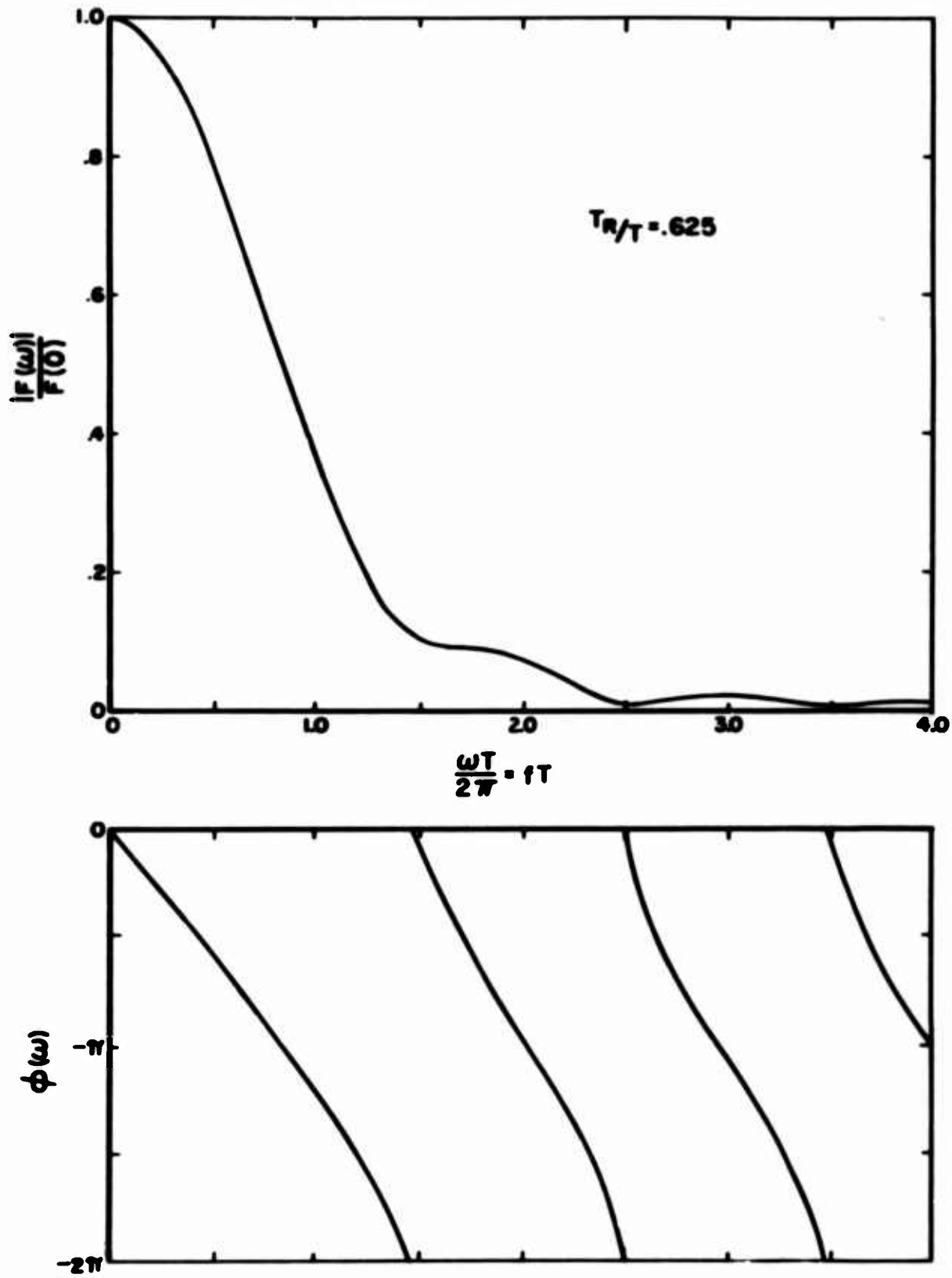


Figure 19. Fourier Amplitude and Phase Spectra for $T_R/T = .625$

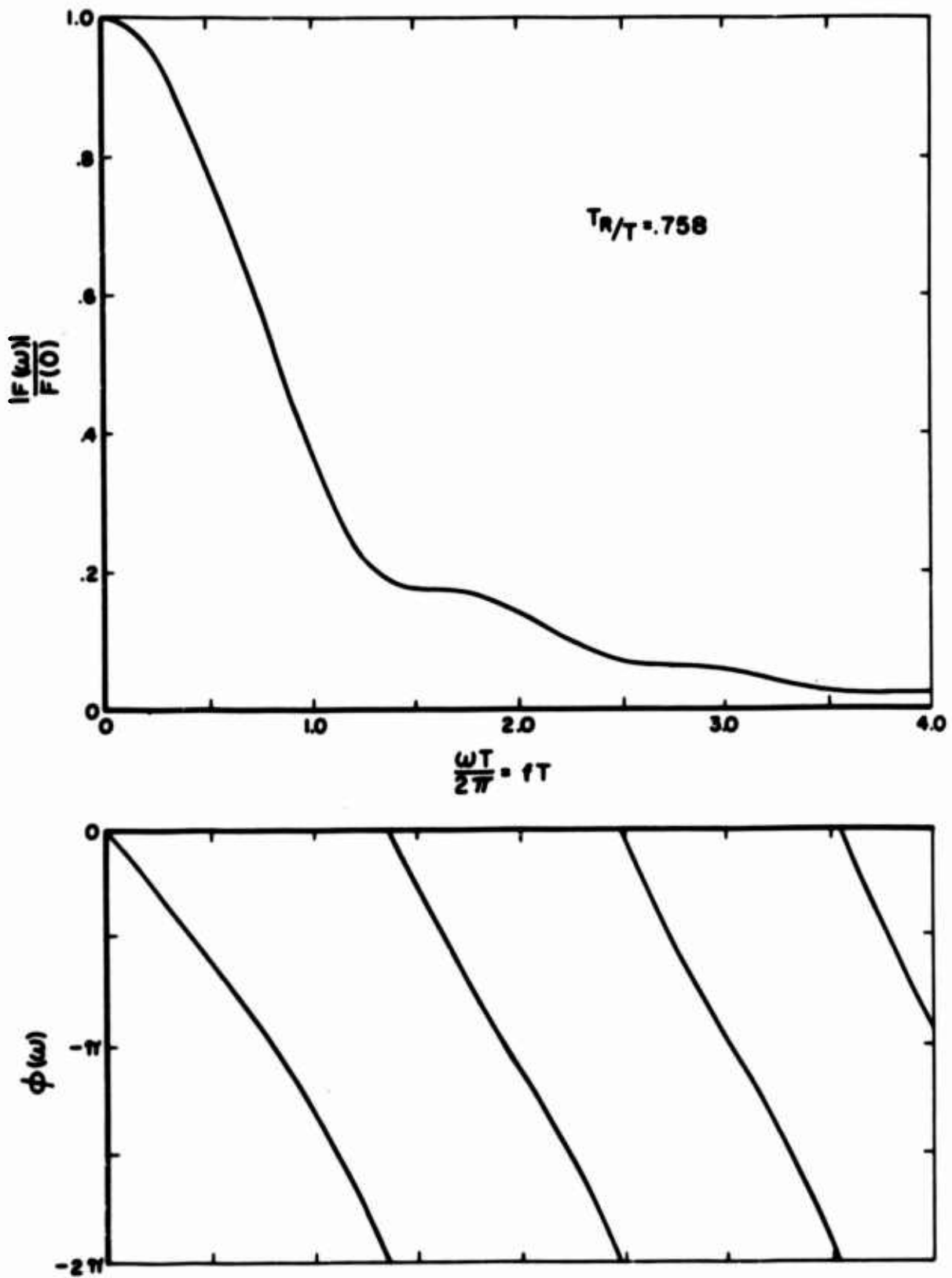


Figure 20. Fourier Amplitude and Phase Spectra for $T_R/T = .758$

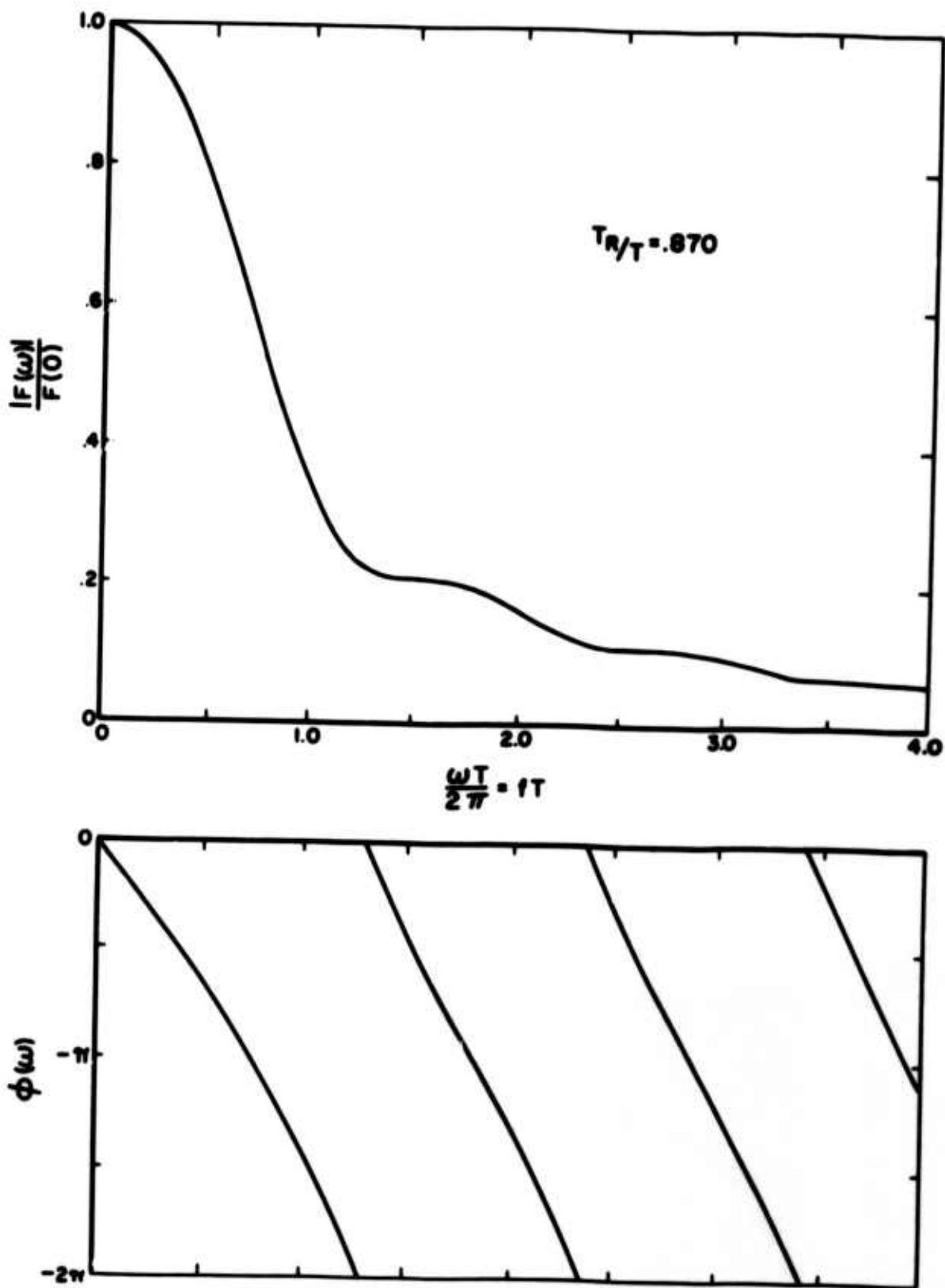


Figure 21. Fourier Amplitude and Phase Spectra for $T_R/T = .870$

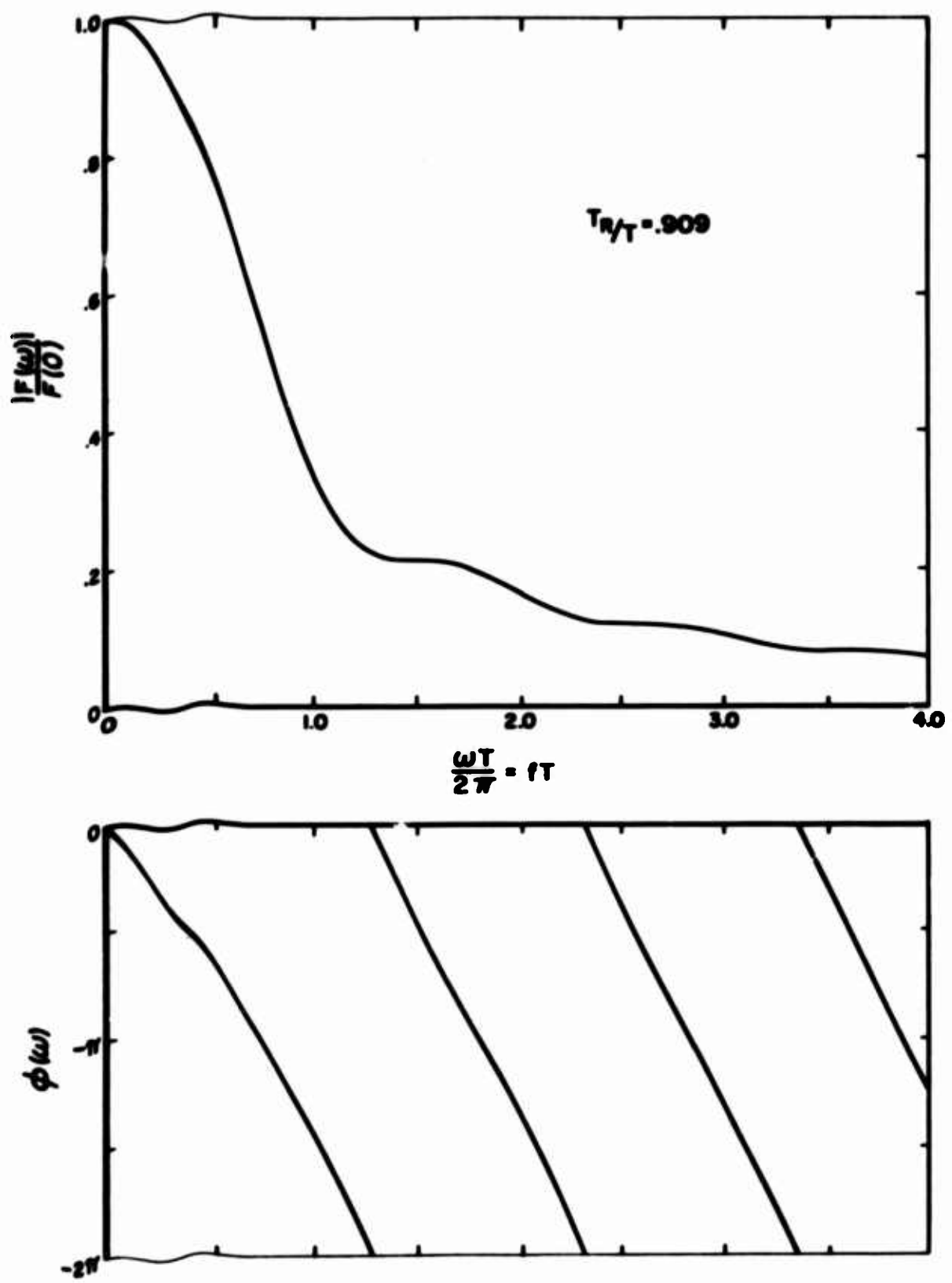


Figure 22. Fourier Amplitude and Phase Spectra for $T_R/T = .909$

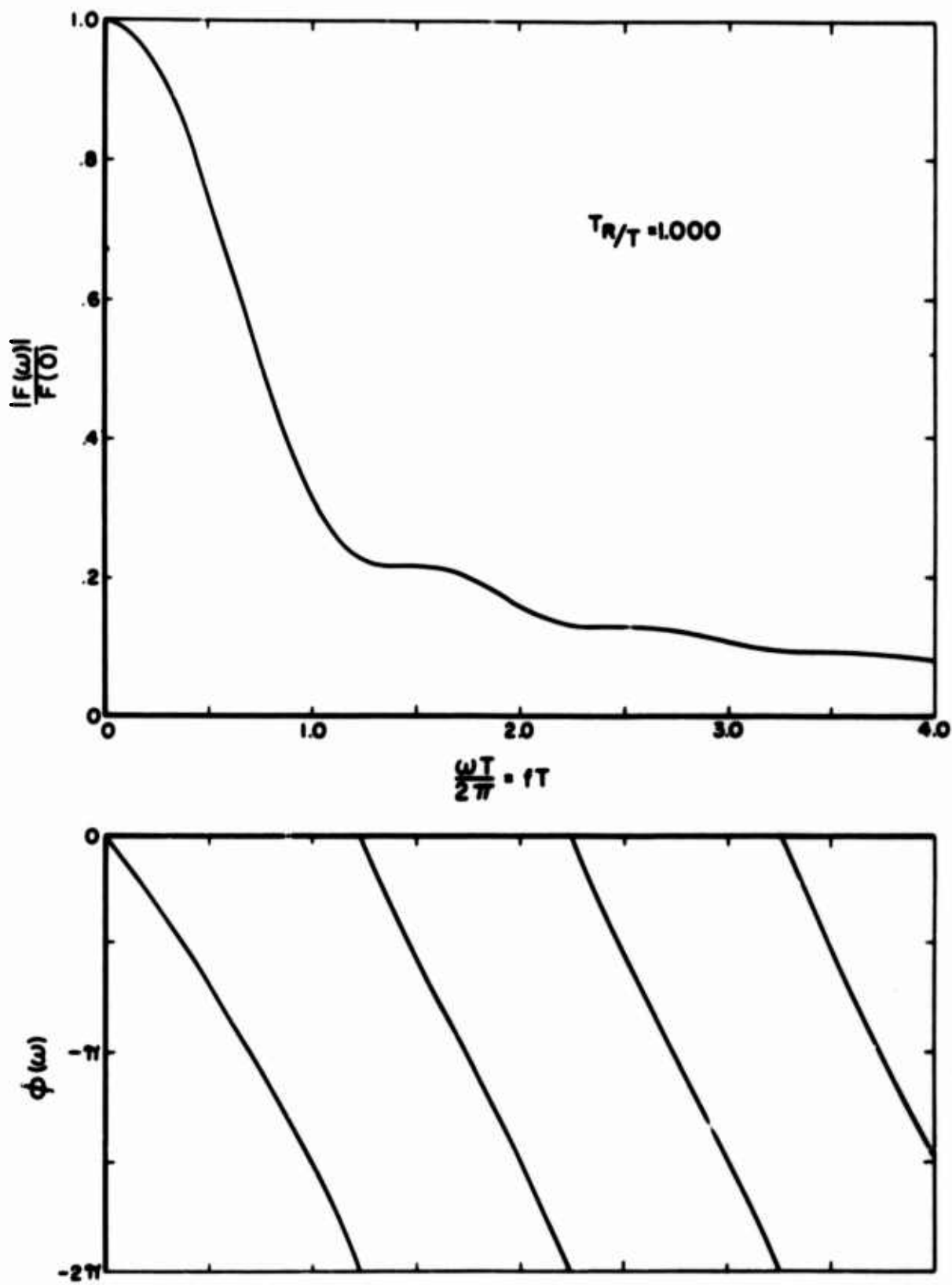


Figure 23. Fourier Amplitude and Phase Spectra for $T_R/T = 1.000$

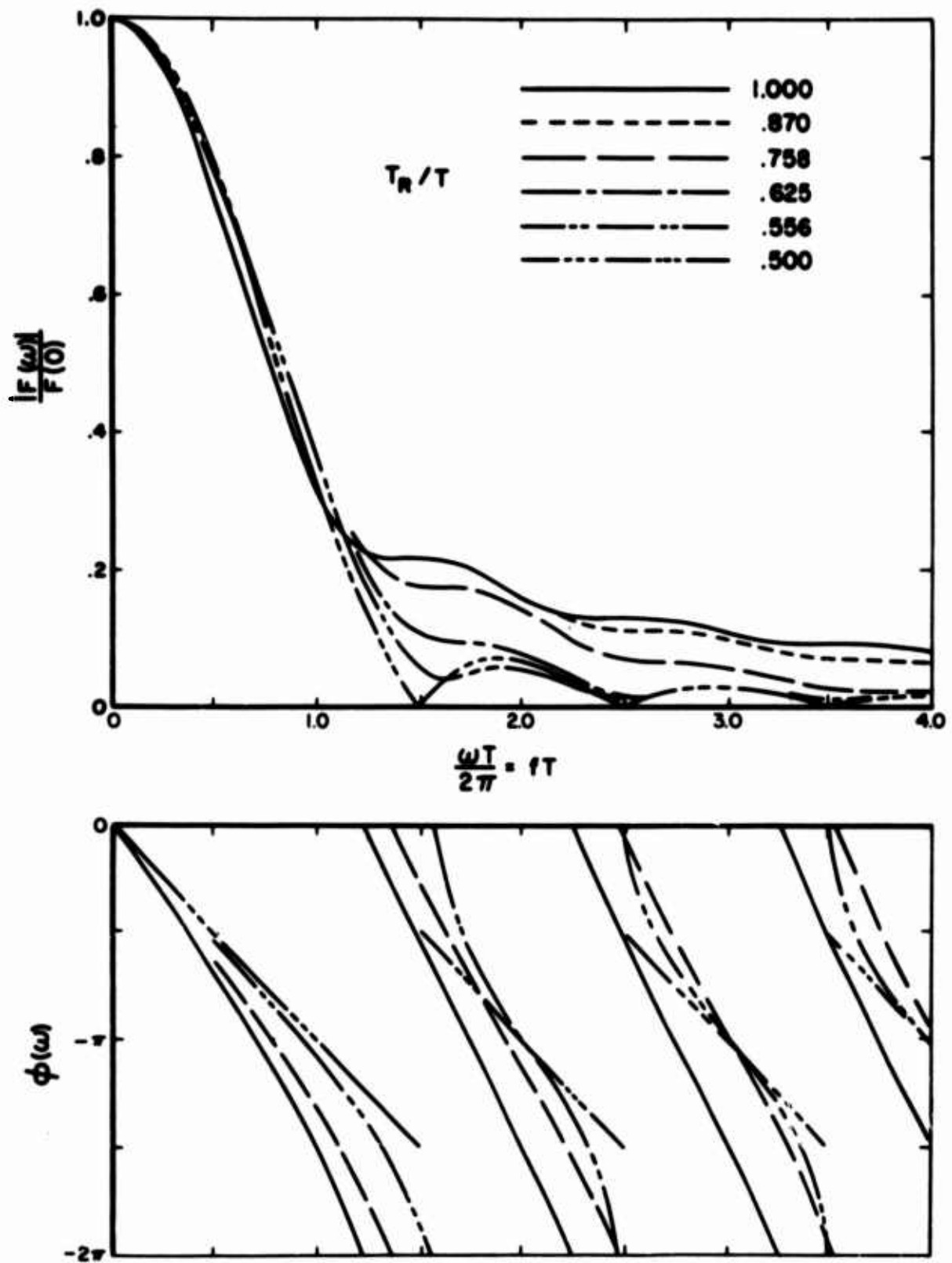


Figure 24. Variations in Fourier Amplitude and Phase Spectra

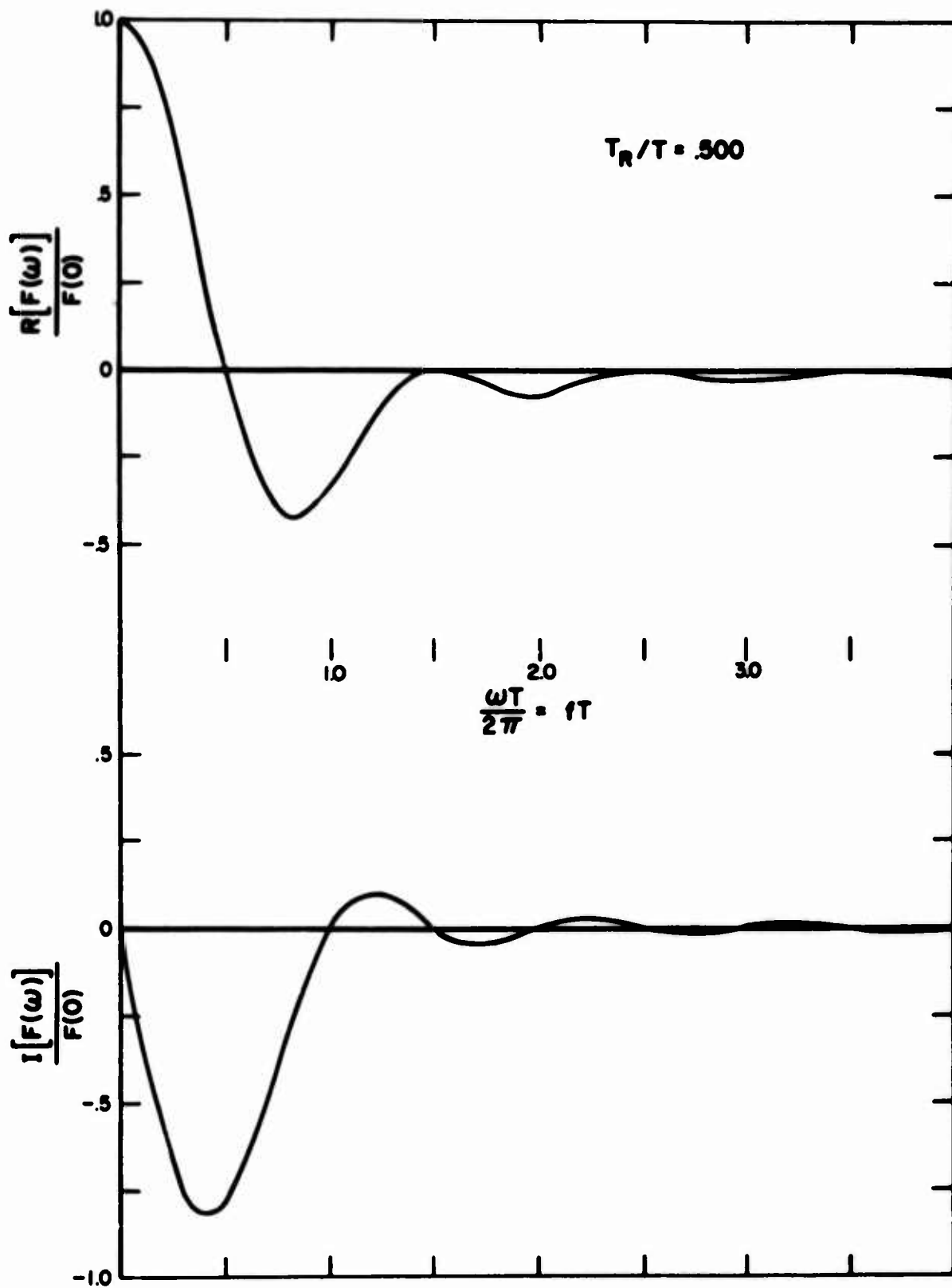


Figure 25. Fourier Real and Imaginary Spectra for $T_R/T = .500$

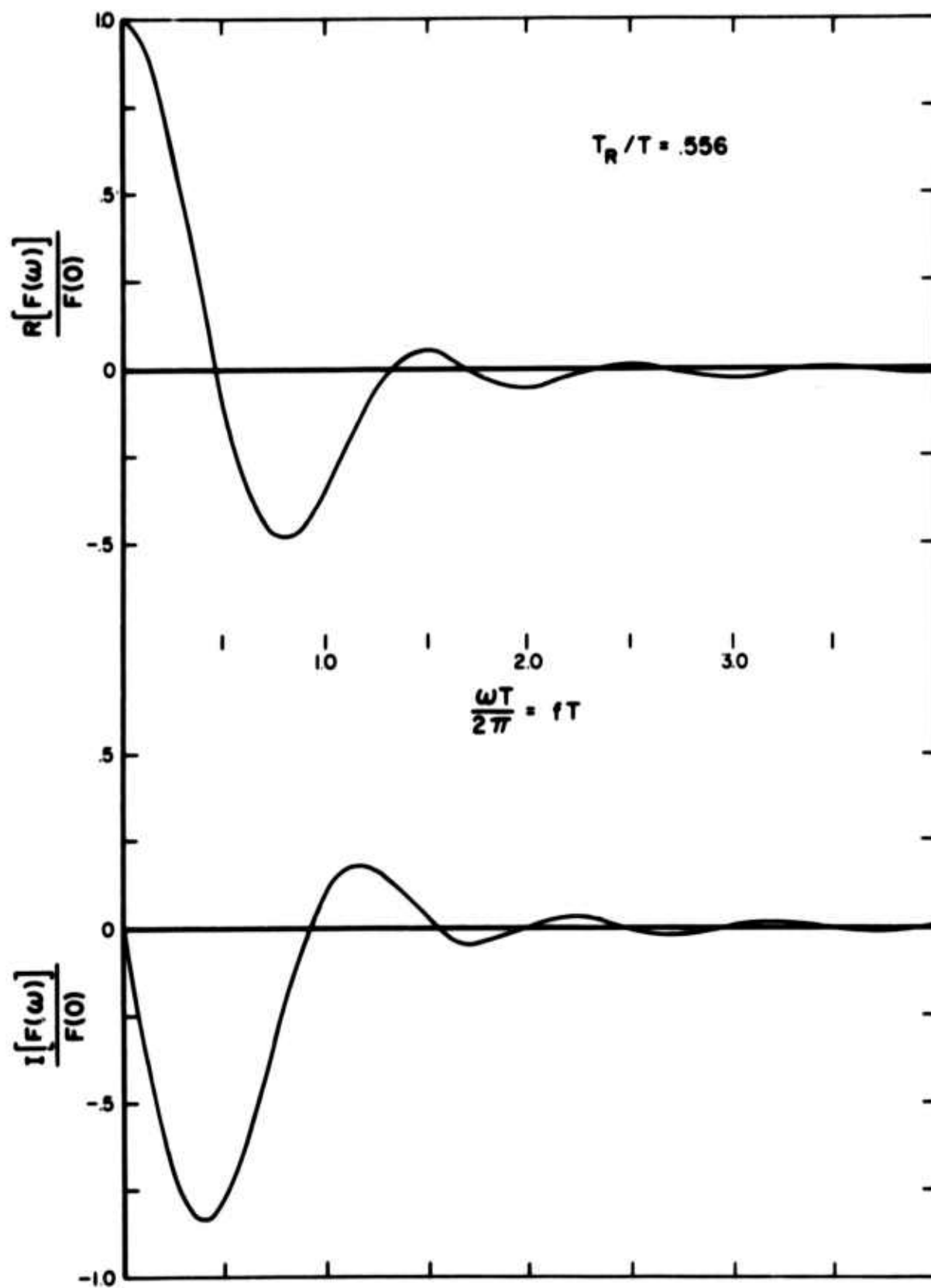


Figure 26. Fourier Real and Imaginary Spectra for $T_R/T = .556$

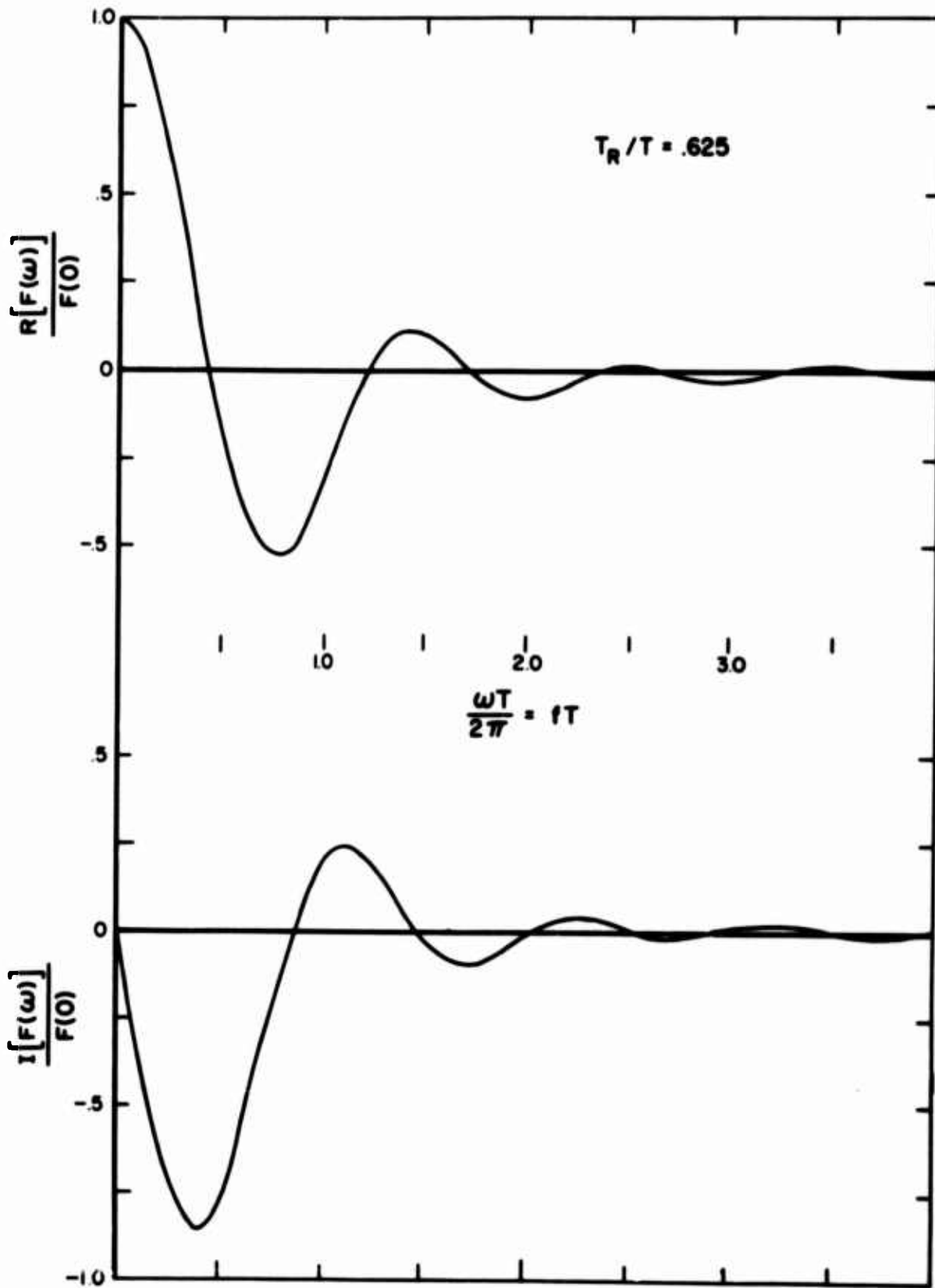


Figure 27. Fourier Real and Imaginary Spectra for $T_R/T = .625$

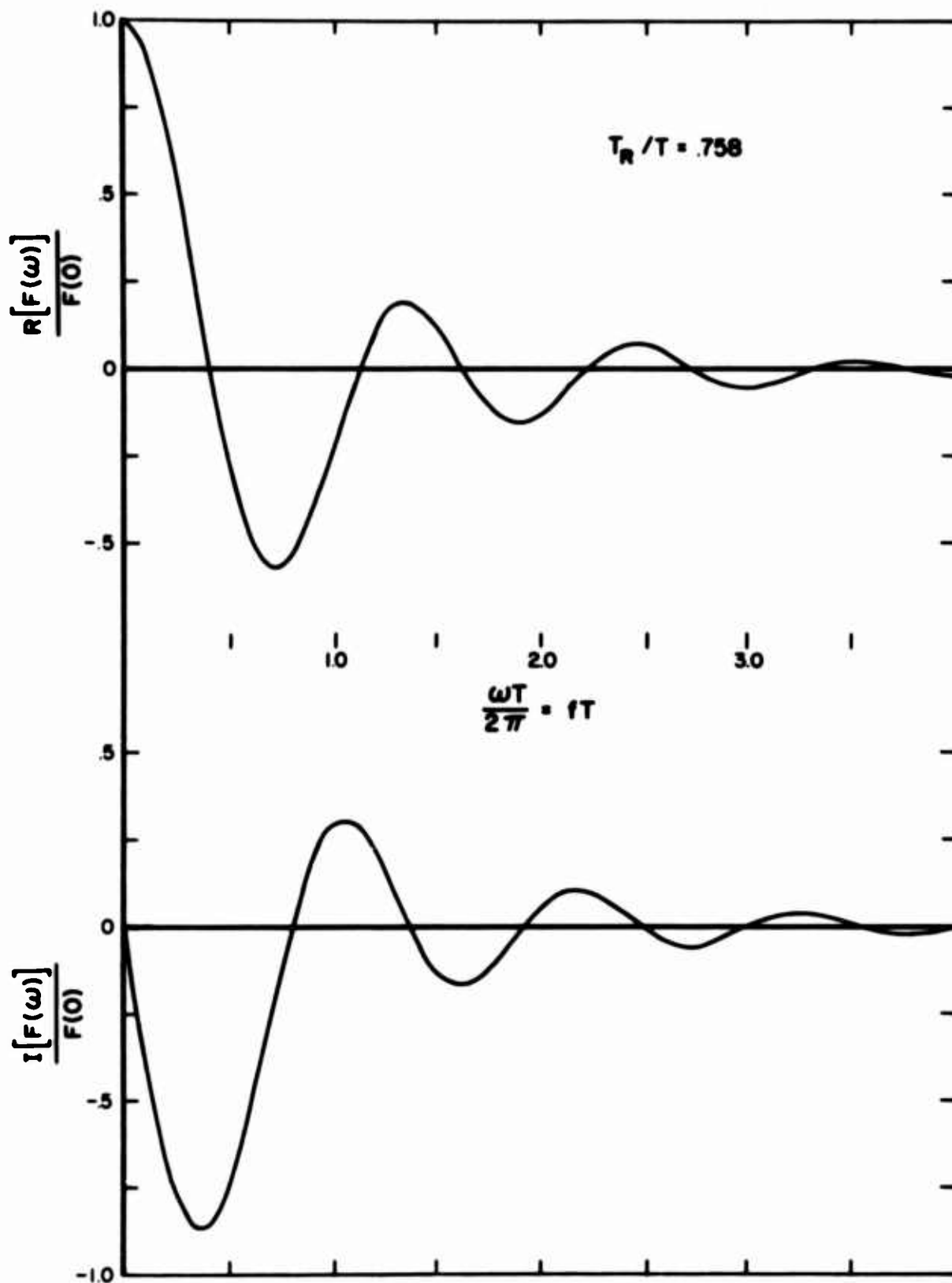


Figure 28. Fourier Real and Imaginary Spectra for $T_R/T = .758$

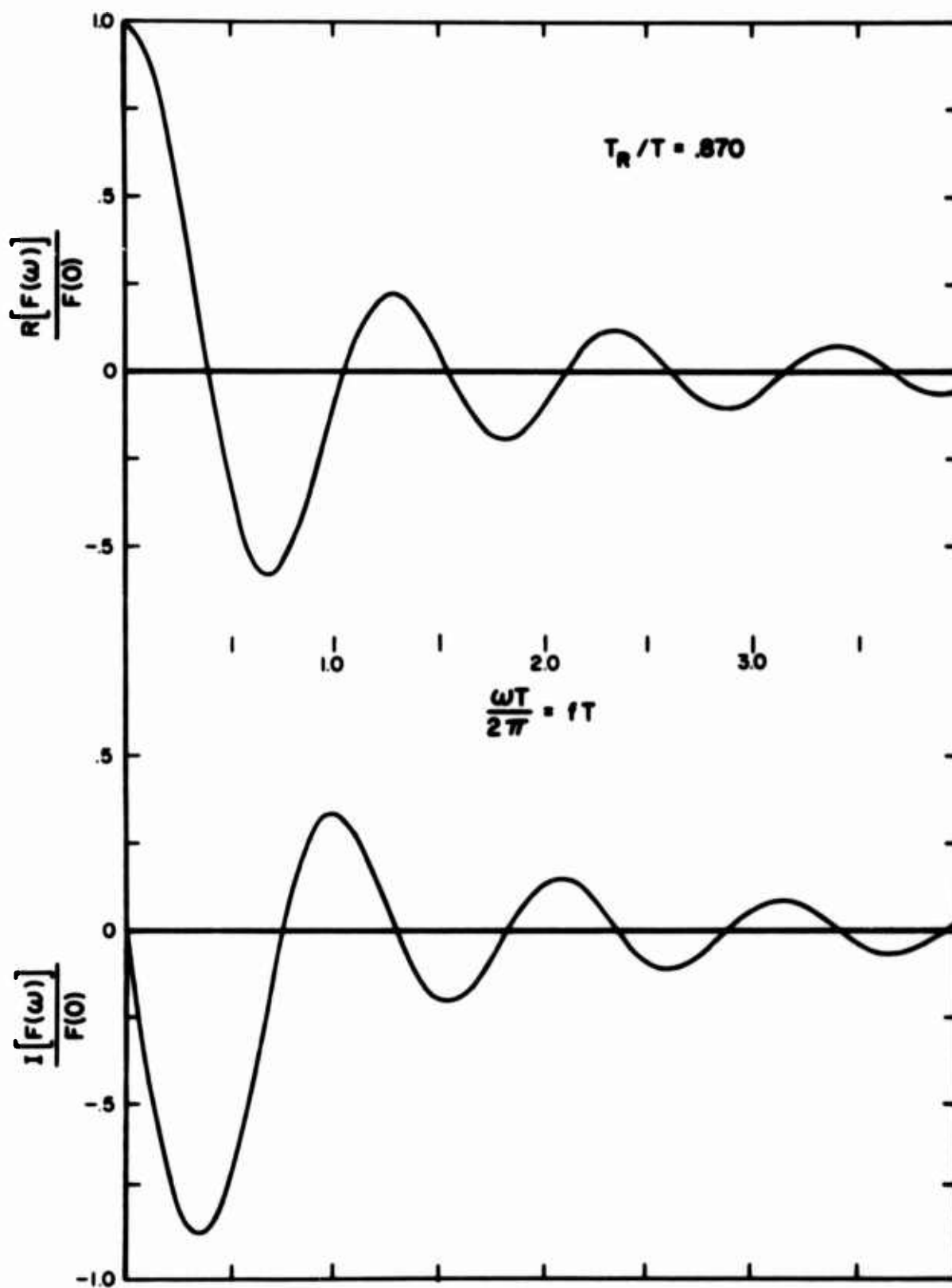


Figure 29. Fourier Real and Imaginary Spectra for $T_R/T = .870$

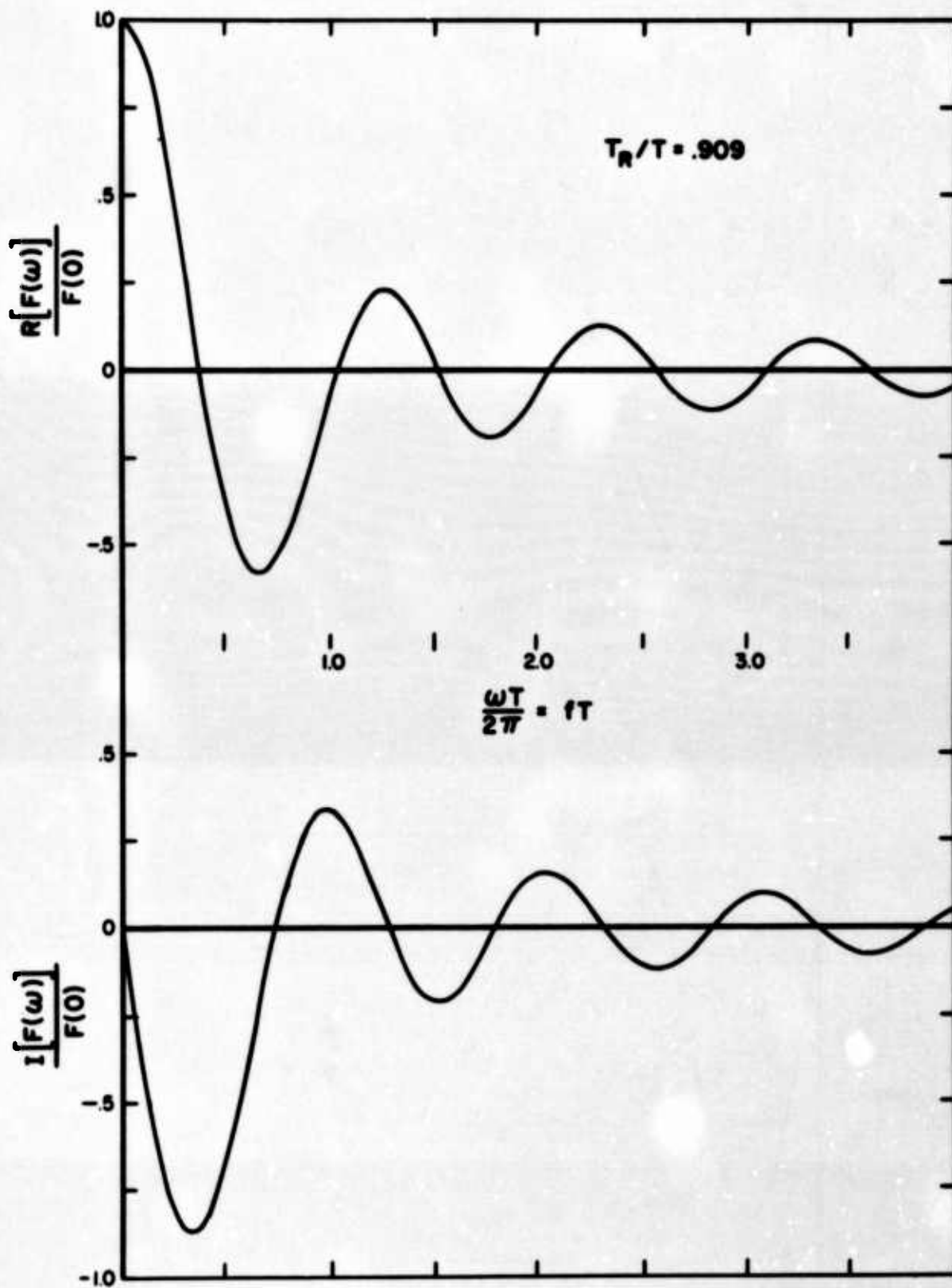


Figure 30. Fourier Real and Imaginary Spectra for $T_R/T = .909$

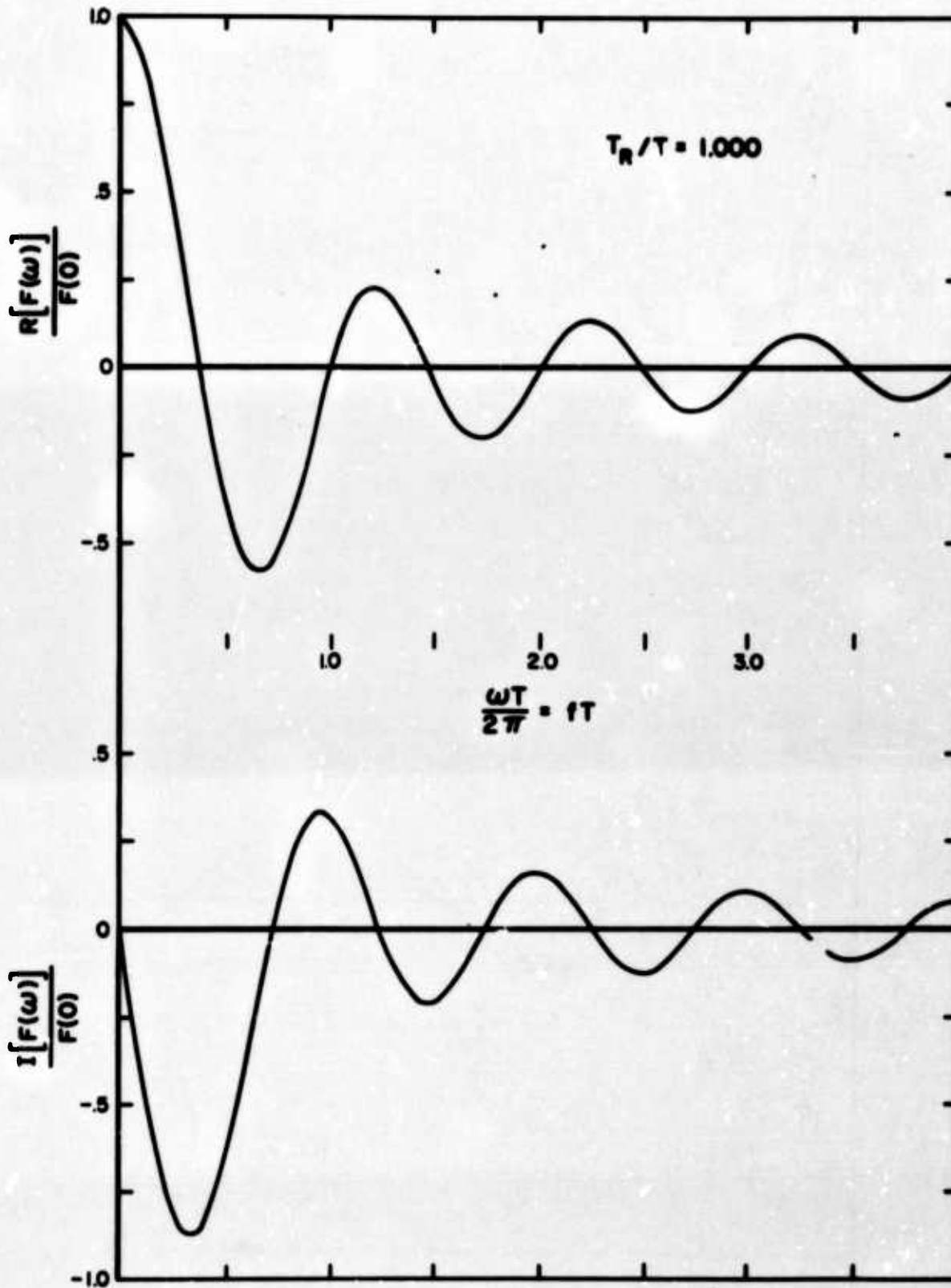


Figure 31. Fourier Real and Imaginary Spectra for $T_R/T = 1.000$

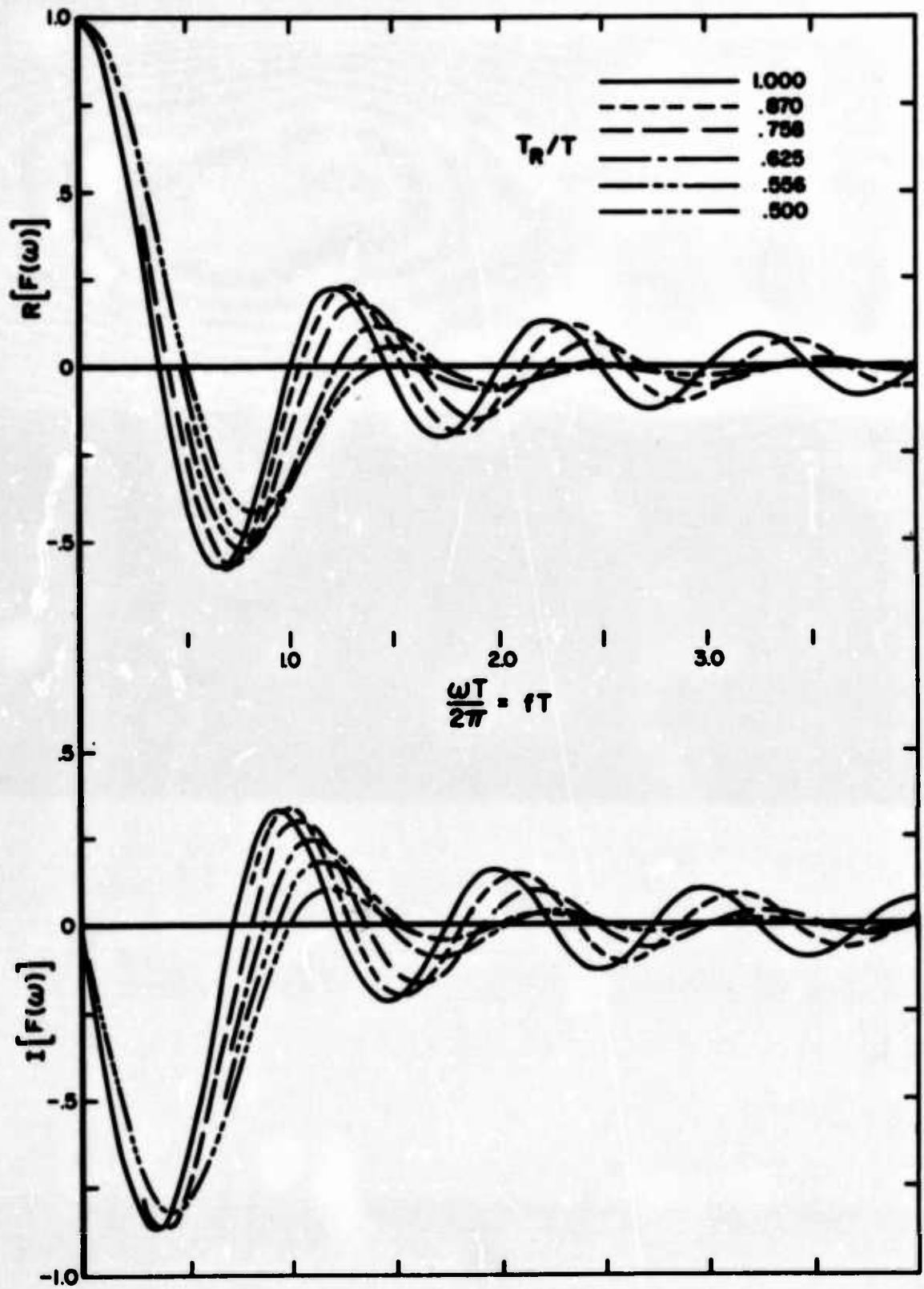


Figure 32. Variations of the Fourier Real and Imaginary Spectra

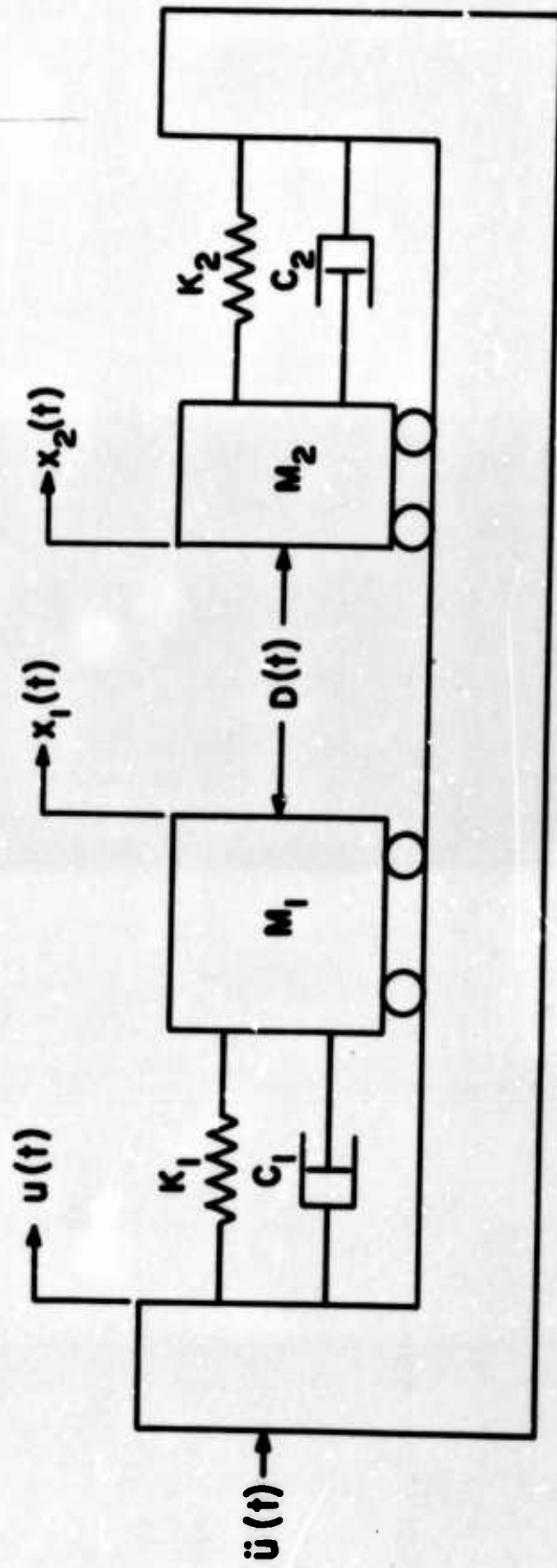


Figure 33. Model Equipment for Determining Proximity Failure Criteria for a Given Excitation

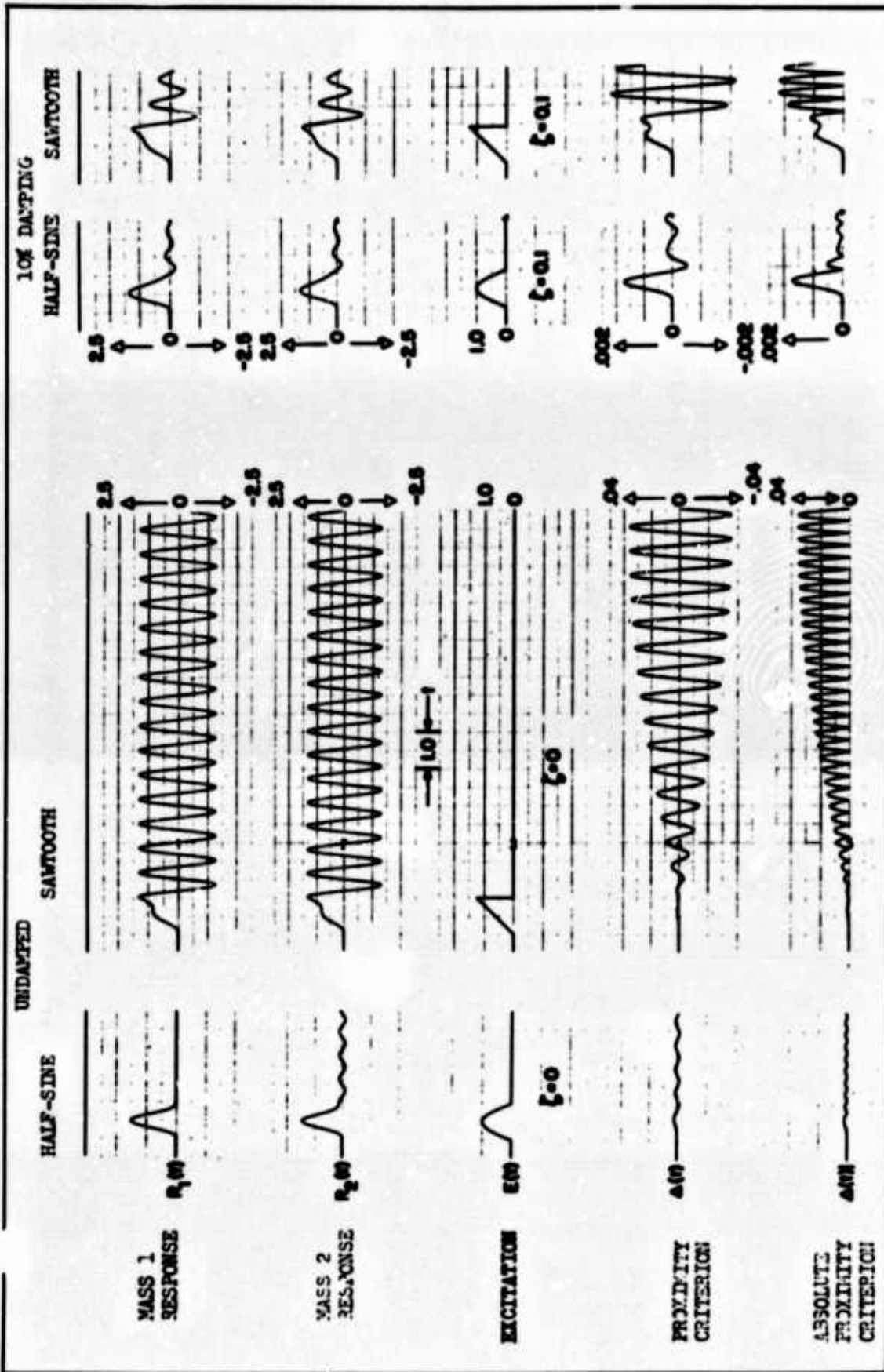


Figure 34. Proximity Criteria for Half-Sine and Sawtooth Pulses When the Half-Sine Criterion is Near Zero

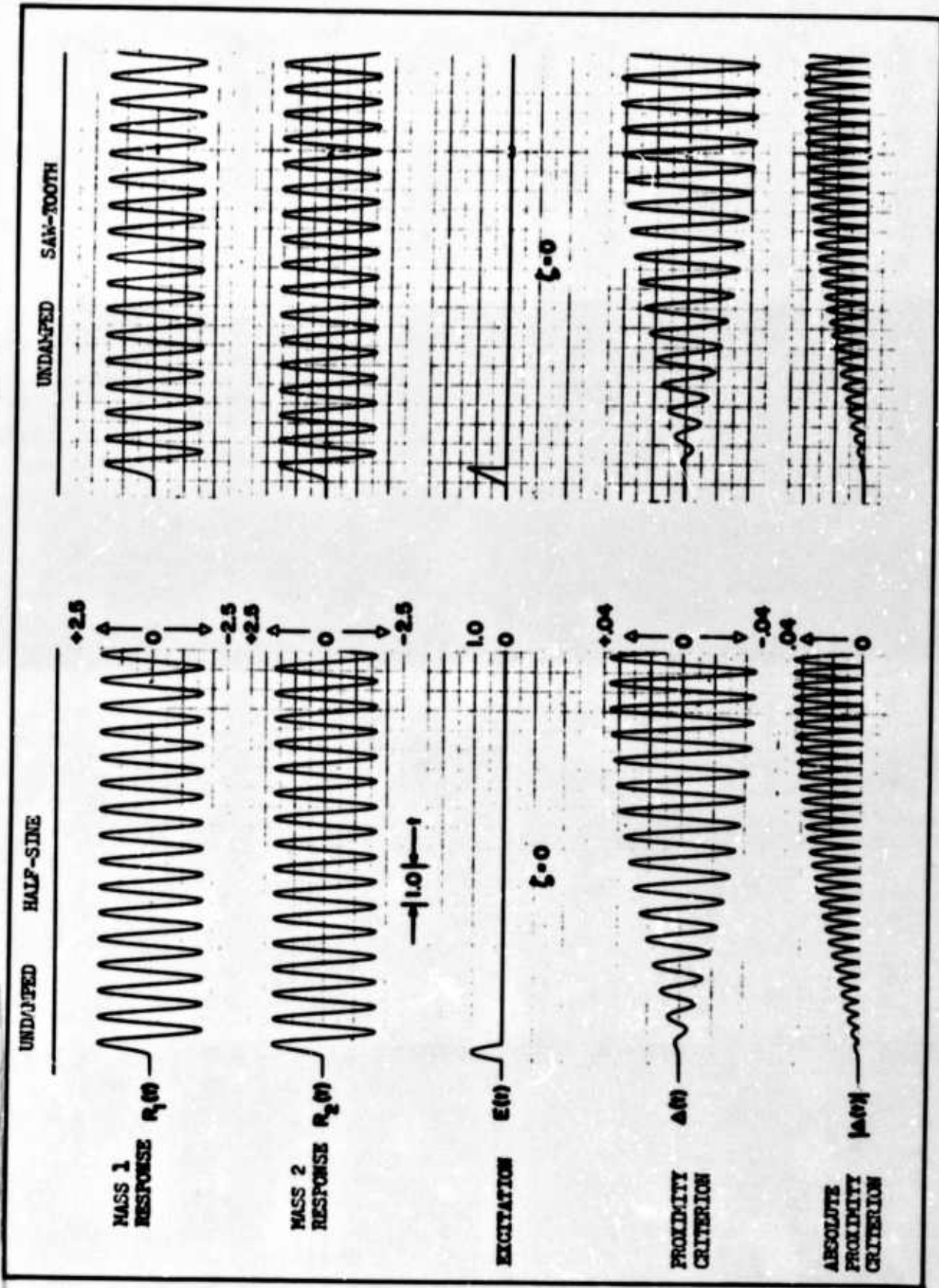


Figure 35. Proximity Criteria for Half-Sine and Sawtooth Pulses When the Half-Sine Criterion is Near Maximum